Evaluation of Spatial Distribution and Temporal Trend of Air Pollution: A Comprehensive Ward-Level Assessment of Dhaka City

Fardeen Shakur Athoye[a, *], Dr. Mohammad Shakil Akther[a]

[a]*Department of Urban and Regional Planning, Bangladesh University of Engineering and Technology (BUET), Dhaka-1000*

***Corresponding Author.**

Fardeen Shakur Athoye,
Department of Urban and Regional Planning, Bangladesh University of Engineering and Technology (BUET), Dhaka-1000.
Mobile Number: +8801402424158
Email Address: athoye.fardeen@gmail.com

Abstract

Dhaka is consistently ranked as one of the most polluted cities in the world regarding air pollution. This research examined air pollution levels across 94 wards of Dhaka North and South City Corporations from 2019 to 2024 to explore variations in air pollution temporally, ascertain differences in spatial distribution, and identify the wards most vulnerable to air pollution. For temporal and spatial analysis, satellite-derived $PM_{2.5}$, NO_2, SO_2, CO, and O_3 concentration data were gathered from Sentinel-5P Precursor and Global Annual $PM_{2.5}$ Grids. A deductive indexing framework was also established based on pollutant concentrations and vegetation coverage (Normalised Difference Vegetation Index) derived from Landsat 8. The results show a notable increase in the annual average concentrations of $PM_{2.5}$ (1.72%), SO_2 (38.58%), CO (6.86%), and O_3 (5.44%), while NO_2 concentrations experienced a decline (13.71%), with overall pollutant levels peaking in winter. Spatially, $PM_{2.5}$, SO_2, and O_3 peaked in the western wards, whereas NO_2 and CO were higher in the eastern wards. The critical area ranking identified highly degraded areas within transport, residential, mixed, and commercial zones, while agricultural, open spaces, health, and the administrative regions demonstrated better air quality. Environmental degradation hotspots were concentrated in Old Dhaka, key commercial hubs (Motijheel, Tejgaon), and traffic gateways (Gabtoli, Uttara), while greener, institutional areas like Gulshan, Basabo, and Dhaka University exhibited better air quality. The study recommends integrating land use into national air quality standards, adopting seasonal mitigation strategies, implementing ward-specific air quality management, and incorporating air quality indicators into local climate action plans.

Keywords: Criteria Pollutant, Spatial Distribution, Temporal Variation, Critical Area Ranking, Dhaka North City Corporation, Dhaka South City Corporation

1. Introduction

Cities drive global environmental change [1]. More than half of the global population resides in urban areas, and by the middle of the century, this is projected to rise to 68% [2]. Consequently, these areas have been consuming a disproportionate share of resources. This situation can substantially impact the regional or local climate and heighten the susceptibility of urban dwellers to future global climate change [3]. One notable consequence of metropolitan areas on their climate is increased air pollution. Urbanisation and industrialisation intensify air pollution [4], posing serious threats to public health, environmental integrity, and economic stability. Recognizing this urgent issue, developed nations in the

USA and Europe have made significant progress in decreasing reliance on fossil fuels and improving air quality between 2005 and 2015 [5], [6], [7], [8]. China has also implemented strict pollution control measures through the Five-Year Plan (FYP 2011–2015), which have proven effective in the East Asian region in reducing air pollutants [9], [10]. However, developing countries, especially South Asian countries, face grave challenges with air pollution due to unregulated urban expansion [11]. Nine of the ten cities with the most severe air quality issues are in this region [12]. Pollution levels in these countries surpass acceptable limits by as much as 20 times compared to what the WHO deems healthy (15 μg/m³) [12], affecting about 86% of populations in countries such as China, India, Pakistan, and Bangladesh with particulate matter (PM) pollution levels above 75μg/m^3 [13].

During the last two decades, heavily industrialized and inadequately planned urban regions of Bangladesh, particularly Dhaka, have experienced degraded air quality [14]. The Global Liveability Index 2018 designated Dhaka as the second least liveable city worldwide because of its severe air pollution [15]. A study on air quality in the world's most polluted 50 cities found that Dhaka is the second most polluted city in the world, with an average annual $PM_{2.5}$ level of 97.1 μg/m^3 (6.5 times higher than the WHO standard) [16]. The Air Quality Index (AQI), scaled from 0 to 500, is a quantitative measure of air quality, with values exceeding 300 classified as hazardous air quality [17]. In 2024, Bangladesh was identified as the leading country worldwide for the highest AQI levels, with Dhaka experiencing good air quality for only 13 days out of 365. For the remaining days, the AQI levels consistently fell within high categories [18]. In January 2025, Dhaka's AQI soared to alarming heights, exceeding 300 and peaking at 367 on the morning of January 22 [19]. The Air Quality Monthly Report for January 2025, released by the Department of Environment (DoE), Bangladesh, classified 24 of the 31 days in January as 'very unhealthy' or 'extremely unhealthy' [20]. These alarming statistics highlight the growing complexity of air pollution in Dhaka. The distribution of air pollutants in terms of space and time plays a crucial role in identifying potential sources of pollution and monitoring changes in air quality levels.

Six pollutants (i.e., PM, SO_2, NO_x, O_3, CO, and Pb) are termed as the criteria air pollutants (CAP) for their abundance as pollutants in the atmosphere [17]. Several studies have examined the spatial and temporal distribution of criteria pollutants such as NO_2, SO_2, CO, and O_3 in addition to $PM_{2.5}$ and PM_{10} in different cities of the world [21], [22], [23], [24], [25], [26], [27], [28], [29]. [28] analyzed air quality indices and pollutant levels across 336 Chinese cities from 2014 to 2019, revealing a decrease in pollutants due to adequate emission controls implemented since 2014. These findings were supported by [24], which noted a drop in annual mean concentrations of several pollutants in China, though NO_2 and O_3 levels showed an upward trend. In Bangladesh, fewer studies have focused on all criteria pollutants; however, findings suggest that most pollutants at ground monitoring stations remained within Bangladesh National Ambient Air Quality (BNAAQS) standards, except for $PM_{2.5}$ and PM_{10}, with annual averages surpassing the standards set by the BNAAQS, the United States Environmental Protection Agency (USEPA), and World Health Organization (WHO) guidelines [13], [30]. [30] also noted instances where NO_2 concentrations either were close to or exceeded the limit values, emerging as another concerning pollutant alongside particulate matter. Studies also reported a declining trend in annual particulate matter concentrations in Dhaka between 2014 and 2017 [13], [31], attributed to ongoing governmental reforms and increased awareness, such as banning two-stroke engines and green technology for brick construction [32], [33].

Although the spatial distribution of air pollutants varies country-wise, they exhibit a common characteristic. The highest concentrations of contaminants and the worst levels of air quality are found to be in urban centres [34], [35], relatively developed and populous areas [23], [36], [37], and areas with high industrial emissions [36]. South Asian regions, including Bangladesh, Pakistan, and India,

are experiencing an increasing air pollution trend due to the lack of rigorous air pollution control policies [38]. Spatial distribution of air pollution across Bangladesh showed substantial regional variations. Hot spots of air pollutants are clustered around major metropolitan areas of Bangladesh, including Dhaka and its surroundings [13], [30], [34], [39], [40]. The southern peripheral regions of Dhaka are undergoing noticeable changes, with Narayanganj and Gazipur recognized as the most polluted areas near Dhaka [13], [30]. Relatively lower air pollutant concentrations are observed in Barisal, Rangpur, and Rajshahi [34], [39].

Air pollution levels exhibit temporal variation influenced by seasonality [13], [21], [23], [36], [40], [41], day of the week [13], and diurnal changes [13], [40]. These studies show higher pollution levels during winter and lower levels during monsoon seasons. This variation is primarily due to seasonal shifts in major local sources of pollution, such as brick kilns and industries. For instance, the increased demand for heating during winter in China led to higher coal consumption, resulting in elevated winter pollutant concentrations [36]. [13] highlighted that in Dhaka, SO_2 levels increase in winter due to the seasonal operation of brick kilns exclusively during the dry season, as rain disrupts the brick production process in the monsoon. Meteorological factors, particularly wind speed, influence these seasonal variations, enabling transboundary pollution from north and northeast directions [42]. Besides, it was also found that $PM_{2.5}$ concentrations peak on Fridays and PM_{10} on Wednesdays, while gaseous pollutants (NO_2, SO_2, CO) show minimal daily fluctuation, likely due to consistent traffic flow throughout the week [13]. Diurnally higher levels of SO_2, NO, CO, $PM_{2.5}$, and PM_{10} are recorded at night, driven by emissions from long-distance buses and heavy-duty diesel trucks [13].

Research also indicates that various events, including strikes, religious festivals, and pandemics, can affect air pollutant levels [25], [26], [43]. Reductions in NO_2, SO_2, PM_{10}, $PM_{2.5}$, and O_3 were observed in Delhi, Mumbai, Thane, Pune, Kolkata, Chennai, Hyderabad, and Ahmedabad, where concentrations were high before the lockdown was imposed during the COVID-19 pandemic [26], [42]. These results were similar to a study on air quality levels in Bangladesh by [44], which documented significant decreases in NO_2, SO_2, O_3, and CO levels across Gazipur, Dhaka, and Chattogram. [25] discovered that during Diwali days, NO_2, SO_2, CO, and O_3 concentrations were approximately 1.5 to 7 times the National Ambient Air Quality Standards (NAAQS) limits over major cities in India. In Dhaka, all pollutants except CO concentration decrease on strike days, with NO_x decreasing on Eid day and remaining lower for the following few days as vehicular movements decrease during Eid festivals in the capital [45].

Despite growing attention, most air pollution research in Dhaka adopts a citywide or regional analyst scale [13], [34], [38], [39], often tackling a single pollutant such as $PM_{2.5}$ [31], [32], [42] or Covid-19 period impacts [45]. By doing this, they possibly overlook the crucial intra-urban variation in pollution exposure that is central to formulating targeted mitigation policy and protecting vulnerable populations. In particular, ward-level disparities in Dhaka remain understudied despite their potential to reveal localized pollution hotspots and inform spatially targeted interventions. Moreover, there have been few investigations that have simultaneously examined multiple criteria air pollutants ($PM_{2.5}$, NO_2, SO_2, CO, O_3) along both spatial and temporal dimensions at a fine urban scale. While satellite-based methods have been used in air quality estimation for other global megacities, the integration of multi-source high-resolution satellite data for the estimation of pollutant impacts at the ward level for Dhaka represents a methodological gap addressed by this study. Mapping air quality, which includes all pollutants, would benefit residents and vulnerable communities in assessing safe areas.

To fill these gaps, this study conducts a ward-level, multi-pollutant air quality analysis in Dhaka for 2019-2024. It analyzes annual and seasonal trends of five criteria pollutants, maps spatial distribution in 94 wards of Dhaka North and South City Corporations, and outlines cumulative impact zones through

mapping environmentally critical wards to identify targeted interventions locally. By redirecting the analytical focus from city-wide averages to intra-urban inequalities and by incorporating numerous pollutants within a cumulative risk paradigm, this research provides a policy-directed contribution to urban environmental planning for one of the world's most contaminated metropolises. This approach is intended to support policymakers of Dhaka city, offering evidence-based recommendations for targeted interventions based on identified hotspots. Moreover, this research aligns with global efforts to achieve the United Nations Sustainable Development Goals (SDGs), particularly SDG 11 (Sustainable Cities and Communities) and SDG 13 (Climate Action), reinforcing its broader relevance.

2. Materials and Methods

2.1 Study Area Description

The Dhaka Metropolitan Area (DMA) lies between 23°41'46.22"N to 23°53'6.3"N latitude and 90°24'9.34" E to 90°24'6.17" E longitude. The DMA is administered under the jurisdiction of two City Corporations: Dhaka North City Corporation (DNCC) and Dhaka South City Corporation (DSCC) [46]. DSCC is subdivided into 10 zones, with 75 wards covering an area of 109.251 km^2 [47]. DNCC is also divided into 10 zones and governs 54 wards covering an area of 196.22 km^2 [48]. The shapefiles delineating the boundary of the study area were obtained from RAJUK (City Development Authority, Dhaka), containing 94 ward polygons, with 34 belonging to the DNCC and 57 to the DSCC, as illustrated in Figure 1. A few areas fall under neither of the two parts and hence are not considered for the study, e.g., Dhaka Cantonment. The city is surrounded by four rivers: Buriganga, Turag, Tongi, and Balu. The annual population growth rate in Dhaka's urban centre stands at 1.79%, which exceeds the national average of 1.12% [49]. Dhaka is increasing vertically and horizontally due to this population expansion, primarily due to rural-urban migration and partly due to natural growth [50]. This economic hub of the country is identified as the third most polluted megacity globally [51].

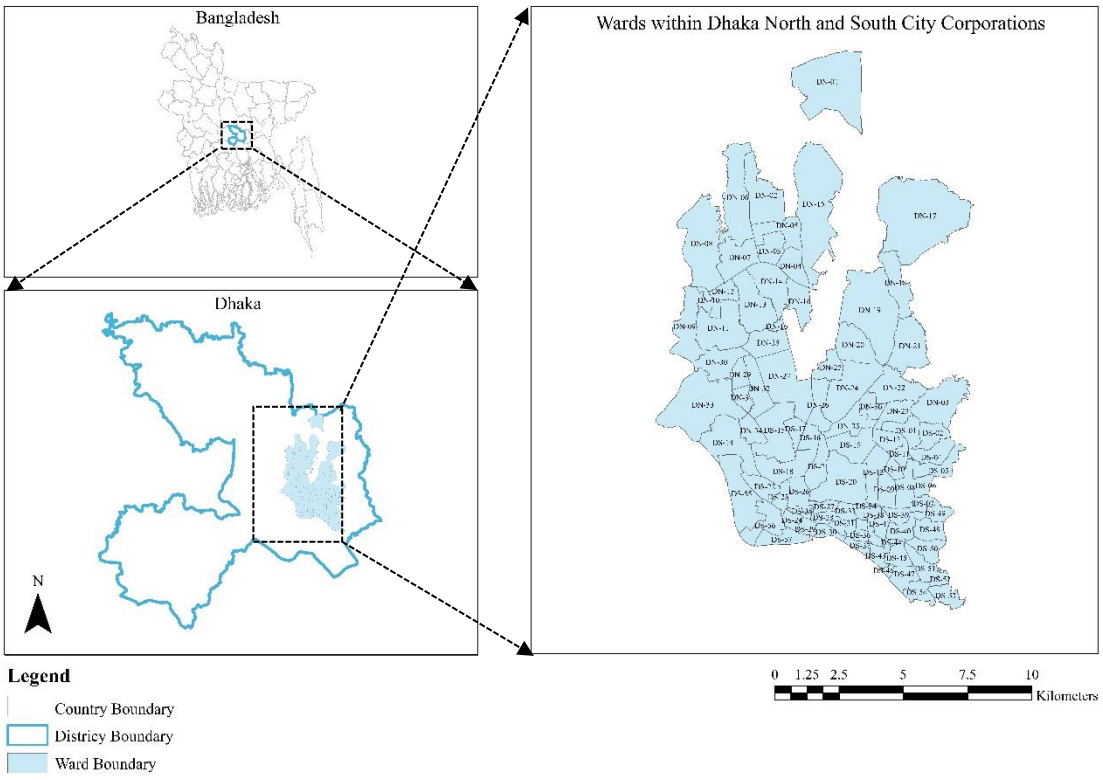

Figure 1 Geographical location of the study area, with a detailed ward-level map of Dhaka North and South City Corporations, highlighting 94 administrative wards considered in the analysis

2.2 Data Collection

Most studies on air pollution have relied on ground-based monitoring stations to collect pollutant data [13], [30], [31], [52], [53], [54], [55], [56]. While these stations offer more precise measurements, they are costly and not sufficiently dense, particularly in South Asia, to accurately assess the spatial distribution of air pollutants [57]. In Bangladesh, there are 11 continuous air monitoring stations (CAMS), with three in Dhaka, which are inadequate for capturing the wide range of pollution levels in urban settings. Using satellite sensor-based systems has proven effective in accurate and almost real-time measurements of pollutants such as $PM_{2.5}$, CO, SO_2, NO_2, CH_4, and CO_2 cost-effectively [58]. Various studies have employed Sentinel-5 Precursor TROPOMI imagery to gather data on NO_2, CO, SO_2, and O_3 [44], [59], [60], [61]. The Sentinel-5 Precursor TROPOMI has been effectively used for monitoring various pollutants due to its capability to capture significant wavelengths and high spatial resolution (0.01 arc degrees), making it suitable for metropolitan air quality assessments. Besides, satellite retrieval of $PM_{2.5}$ is also a cost-efficient alternative for $PM_{2.5}$ monitoring at a sizeable spatiotemporal scale [43]. The study utilises satellite-derived remote sensing images to analyse air pollution patterns from 2019 to 2024 (Table 1). The study also considered the influence of seasonal variations on pollutant levels. The winter season in Bangladesh ranges from December to February, summer from March to May, and monsoon from June to September [62], [63], following which the seasonal air pollutant data were categorised.

Table 1 Key specifications of the data utilised in this study

Data Source	**Parameter**	**Spatial Resolution**	**Temporal Resolution**	**Default Unit***
Sentinel-5P TROPOMI	Nitrogen Dioxide (NO_2), Sulphur Dioxide (SO_2), Carbon Monoxide (CO), Ozone (O_3)	1113.2m×1113.2m	Daily	mol/m^2
Global Annual $PM_{2.5}$ Grids	$PM_{2.5}$	0.01°×0.01°	-	$\mu g/m^3$
Landsat 8	Normalised Difference Vegetation Index (NDVI)	30m×30m	Daily	-
RAJUK Geodatabase	Administrative Boundary, Physical Features	-	-	-

*Default units are the units as obtained from the satellite/reanalysis image

High-resolution offline images from the Google Earth Engine (GEE) repository were utilised to collect NO_2, SO_2, O_3, and CO data. The vertical column density (mol/m^2) is the physical quantity of the air pollution unit. The Level 2 Sentinel-5P TROPOMI products provide an original sensor resolution of 5.5 × 3.5 km [64], though they may be compromised by noise and atmospheric interference. All Level 2 products were upgraded to Level 3 using the Harp convert tool to enhance data quality, and the GEE data archives directly facilitated this access. Temporal filters were applied to compile annual and seasonal data for 2019 to 2024. The imageries also underwent spatial filtering by utilising the administrative boundary imported into the system, having been sourced from RAJUK 2014. The filter array was employed after both satellite imagery and shape files. After applying the spatial and temporal filters, all the pollutant products from the interest period were generated. To derive monthly and yearly composites, the mean function in GEE was applied to calculate average pollutant concentrations. This process was conducted separately for each month and year between 2019 and 2014 for each pollutant (NO_2, SO_2, CO, O_3). The data was then exported in GeoTIFF format to Google Drive for further GIS analysis.

NASA Socioeconomic Data and Applications Centre (SEDAC) at Columbia University provides access to Global Annual $PM_{2.5}$ Grids from MODIS, MISR, and SeaWiFS Aerosol Optical Depth (AOD), v4.03 (1998–2022). This dataset includes $PM_{2.5}$ concentration values (μg/m^3) per 0.01° grid cell, available in raster-ASCII and GeoTIFF formats [65]. For this study, the annual average data of $PM_{2.5}$ were collected in raster-ASCII format with a 0.01° × 0.01° high spatial resolution between 2019 and 2022. The data are available in GeoTIFF format in the WGS84 projection as downloadable zip files and can be directly used in mapping and geospatial analysis [65]. Due to data availability constraints, seasonal data on $PM_{2.5}$ could not be collected for this study. [66] developed global fine $PM_{2.5}$ concentration estimates from 1998 to 2014, utilizing satellite data sources like AOD from various products and ground-based sun photometer observations. Their approach, featuring a Geographically Weighted Regression (GWR) technique, yielded a strong consistency (R^2 = 0.81) compared to cross-validated $PM_{2.5}$ monitor data. While the dataset facilitates large-scale studies, it faces challenges in accuracy, especially in Central Asia and North Africa, due to limited ground monitoring stations [65]. Studies have effectively utilised this data to explore $PM_{2.5}$ variations in South Asia, with the latter confirming a high correlation (R^2 = 92.05%) between data collected from the SEDAC $PM_{2.5}$ archive and ground-based monitoring in the Greater Dhaka [43], [67]. This ongoing research acknowledges the inherent uncertainties in ground-level $PM_{2.5}$ measurements while providing valuable insights into air quality in different wards of Dhaka.

In this study, an environmentally critical area analysis was done between 2019 and 2022 based on air quality and vegetation coverage**.** Landsat images are commonly utilised in remote sensing to determine Land Surface Temperature (LST) and other remote sensing indices (Normalised Difference Vegetation Index, Normalised Difference Water Index) [68]. Due to the higher spatial resolution of the thermal sensors on Landsat compared to other satellites, the study used Landsat 8 images equipped with TIRS thermal sensors for collecting data on vegetation coverage between 2019 and 2022. The United States Geological Survey (USGS) generates remote sensing data in three tiers, with Tier 1 representing data that satisfies both geometric and radiometric quality standards and encompasses raw data. The collected Landsat 8 data for this study comprised images from Collection 2, falling under Tier 1 and Level 2 (Product code: LANDSAT/LC08/C02/T1_L2, consisting of images filtered annually between 2019 and 2022 for the specified years using the GEE code editor.

In addition to the remote sensing data, some secondary data were collected to delineate the study area and to support data analysis. The geodatabase of the Detailed Area Plan (DAP) of RAJUK includes the administrative boundaries and physical features of the DMA. This geodatabase provided polygon shape files of land use and point-shape files of brickfields, CNG and gas filling stations, bus stands and terminals, toll booths, truck stands and terminals, boat ghats, and railway stations. Utilising Arcgis 10.8, these shape files were extracted and incorporated into the study.

2.3 Image Pre-processing and Data Correction

Researchers have used geometric, atmospheric, and radiometric pre-processing techniques [69], [70]. Since USGS had finished geometric corrections on Level 1 products and included atmospherically corrected surface reflectance bands, the focus of the pre-processing was mainly radiometric calibration, transforming the digital number (DN) values of the multispectral bands (bands 1–7 and 9) into surface reflectance values and converting the DN values of the thermal bands (bands 10 and 11) into at-satellite brightness temperature (TB) represented in degrees Kelvin [71]. For the Landsat 8 OLI thermal band, the top of atmospheric radiance (L_λ) is calculated by converting DN values using Eq. 1 provided by [72].

$$L_\lambda = M_L \text{ X } QCAL + A_L \quad \text{.....Eq. 1}$$

Where M_L = multiplicative rescaling factor for specific band (0.0003342),

QCAL = digital numbers of band 10,

A_L = additive rescaling factor for specific band (0.1)

Calibrated images were filtered spatially and temporally and visualised on the GEE interface utilising 'SR_B4', 'SR_B3', and 'SR_B2' bands (representing red, green, and blue bands) to assess cloud cover, which was prevalent across various periods. A cloud masking technique was applied to enhance clarity in the filtered images by removing cloud pixels before extracting green spaces using the NDVI.

NDVI was proposed by [73] to measure green coverage of an area and can be expressed as

$$NDVI = \frac{\rho NIR - \rho R}{\rho NIR + \rho R} \quad \text{.....Eq. 2}$$

Where ρNIR= mean reflectance in the near-infrared channel

ρR= mean reflectance in the red channel.

Since the index is calculated through a normalization procedure, the range of NDVI values is between 0 and 1, having a sensitive response to green vegetation even for low vegetation-covered areas [74].

2.4 Raster Re-gridding for Satellite-derived Air Pollutants

The study combines raster images of NDVI and air pollutants ($PM_{2.5}$, NO_2, SO_2, CO, and O_3). A critical step involved aligning the disparate spatial resolutions of these datasets, as NDVI has a resolution of 30 meters, while the Sentinel-5P air pollutant datasets are at 1113.2 meters. The spatial resolutions of all raster images needed to be aligned to ensure consistency in air pollutant data while maintaining a uniform resolution across the datasets. To achieve consistency, all raster images were resampled to the finest 30m resolution of Landsat 8 as a reference, utilizing bilinear interpolation for accuracy. This interpolation method, which averages the values of the four nearest cell centres, is suitable for continuous data and has proven effective in mapping ambient air pollution [75]. The raster datasets were not defined by the study area boundary and only georeferenced (UGS 1984) but not projected. Cells corresponding to the study area were extracted by masking and projected to UTM Zone 46N, with the assistance of the model builder, for efficiency in repetitive tasks.

2.5 Data Analysis

The mean annual and seasonal concentrations of air pollutants from 2019 to 2024 have been utilised to evaluate the temporal and spatial variation patterns. Regarding $PM_{2.5}$, only the yearly averages between 2019 and 2022 were subjected to analysis. Box plots were prepared to analyse the seasonal distribution of NO_2, SO_2, CO, and O_3 from 2019 to 2024.

Boxplots were also used to identify inconsistent values that exceeded the 1.5 times ± interquartile range. No extreme outliers were found. The Shapiro–Wilk test [76] indicated that the concentrations of NO_2, SO_2, CO, and O_3 across summer, monsoon, and winter seasons did not conform to a normal distribution ($p < 0.05$). There was also a lack of homogeneity of variances, as evaluated by Levene's test ($p < .05$). Given that the data did not meet the assumptions of normality, a Kruskal-Wallis H Test was employed to investigate potential significant differences in pollutant concentrations across the seasons. While this test assessed overall differences, it required a post-hoc pairwise comparison via the pairwise Mann-Whitney U Test to pinpoint specific seasonal variations. All statistical procedures were conducted using the R computing platform at a significance level of 5% ($p = 0.05$).

Air quality mapping is essential for liveable area discovery [77]. A deductive indexing methodology was employed to analyse the cumulative effects of all pollutants [77], [78], [79]. In this context, environmental quality is characterised based on the number of green spaces and air quality status, wherein wards deficient in green spaces and exhibiting elevated pollutant concentrations correspond to

diminished environmental quality. The deductive indexing approach uses an Arcgis raster calculator to calculate ratios of green space area, represented by NDVI, to various pollutant concentrations between 2019 and 2022, including $PM_{2.5}$, NO_2, SO_2, CO, and O_3. The indices, as outlined by [78], are specified in Eq. 3-Eq. 7.

$$Index_1 = NDVI / PM2.5 \quad \text{.....Eq.3}$$

$$Index_2 = NDVI / NO2 \quad \text{.....Eq.4}$$

$$Index_3 = NDVI / SO2 \quad \text{.....Eq.5}$$

$$Index_4 = NDVI / CO \quad \text{.....Eq.6}$$

$$Index_5 = NDVI / O3 \quad \text{.....Eq.7}$$

$$\text{Critical Area Ranking} = Index_1 + Index_2 + Index_3 + Index_4 + Index_5 \quad \text{.....Eq.8}$$

In Eq.8, lower-ranking values reflect highly critical, degraded environments unsuitable for human habitation, while higher values indicate satisfactory conditions. This analysis led to categorising wards into highly degraded, moderately degraded, and lightly degraded, culminating in creating an environmentally degraded area map. This indexing method, which makes use of NDVI and pollutant ratios, could be used as an urban planning tool for Dhaka's air quality management. Besides, it is also possible to adapt the presented methodology to various urban regions in sustainable urban planning initiatives aimed at creating cities with better environments.

Table 2 Annual mean of five criteria pollutants (including $PM_{2.5}$, NO_2, SO_2, O, and O_3) of 94 wards in Dhaka from 2019 to 2024 (Regarding $PM_{2.5}$, concentrations are available between 2019 and 2022)

	$PM_{2.5}$ ($\mu g/m^3$)	**NO_2 ($\mu mol/m^2$)**	**SO_2 ($\mu mol/m^2$)**	**CO ($mmol/m^2$)**	**O_3 ($mmol/m^2$)**
2019	70.87±0.59	183.99±9.63	103.79±23.00	43.13±0.18	117.87±0.07
2020	88.91±3.62	191.18±11.93	14.24±4.14	44.7±0.20	120.72±0.04
2021	90.03±3.39	257.42±17.59	19.79±3.08	45.69±0.20	121.97±0.04
2022	72.09±3.16	264.54±16.02	130.28±36.43	44.47±0.20	124.04±0.03
2023	-	193.37±8.62	162.05±27.69	44.43±0.18	124.29±0.07
2024	-	158.76±13.44	143.83±39.22	46.09±0.43	124.29±0.07
Average	80.47±2.69	208.21±12.87	95.66±22.26	44.71±0.23	122.19±0.03

Values presented as mean ± standard deviation

3. Results

3.1 Temporal Variations in Air Pollution Across the Wards in Dhaka

Temporal variation in Dhaka's air pollution has been analyzed from annual and seasonal dimensions. Mean NO_2, SO_2, CO, and O_3 from 2019 to 2024 were studied for annual variation analysis. However, temporal variation for $PM_{2.5}$ was assessed between 2019 and 2022, as later data were unavailable. This study also examined the variations in air pollution levels across three seasons from 2019 to 2024: summer (March-May), monsoon (June-September), and winter (December-February). The analysis used each pollutant's seasonal mean concentrations, averaged over six years. The results are illustrated through maps and graphs. The maps depict different shades, ranging from blue, indicating low pollution levels, to dark red, indicating high pollution levels.

Table 2 shows the mean concentration of five pollutants in Dhaka from 2019 to 2024, revealing an alarming mean $PM_{2.5}$ concentration of 80.47 µg/m^3. This figure substantially surpasses the national and international standards set by the BNAAQS (15 µg/m^3), the WHO (10 µg/m^3), and the USEPA (12 µg/m^3). The findings are consistent with previous studies in Dhaka [32], the Greater Dhaka Region comprising Dhaka, Narayanganj, Gazipur, Narshingdi [13], and Chittagong [80]. Figure 2 and Figure 3a showed an irregular trend in $PM_{2.5}$ levels between 2019 and 2022, particularly with elevated concentrations in 2020 (88.91 µg/m^3) and 2021 (90.03 µg/m^3). Before the 11th National Parliament Election in 2018, $PM_{2.5}$ levels experienced a substantial rise, largely due to intensified construction activities for major infrastructure projects like the Elevated Metro Line, Bus Rapid Transit (BRT), the Dhaka Elevated Expressway, and the Third Terminal of Hazrat Shahjalal International Airport (HSIA) [31]. However, during the fiscal year 2020, these development initiatives encountered substantial delays owing to the COVID-19 pandemic, which ultimately led to a push for the expedient completion of mega projects before the anticipated general elections in December 2023. Despite pandemic restrictions, construction activities proliferated, exacerbating PM levels that peaked in 2021. Following this peak, $PM_{2.5}$ levels reduced modestly in 2022 (72.09 µg/m^3). According to [81], this decrease marked a reversal of a two-decade trend of increasing pollution in South Asia, where all countries, except Sri Lanka, reported lower $PM_{2.5}$ levels. Bangladesh experienced the most considerable decline, followed by India and Nepal, particularly in districts like Dhaka and Chittagong in Bangladesh, West Bengal, and Jharkhand in India. Favourable meteorological conditions likely amplified the impact of minor reductions in $PM_{2.5}$ and its precursor emissions (SO_2, NO_x, NH_3) across the region. Despite the noted improvement, the annual mean $PM_{2.5}$ concentrations increased by 1.72% from 2019 to 2022, remaining 5-6 times higher than national and international standard limits.

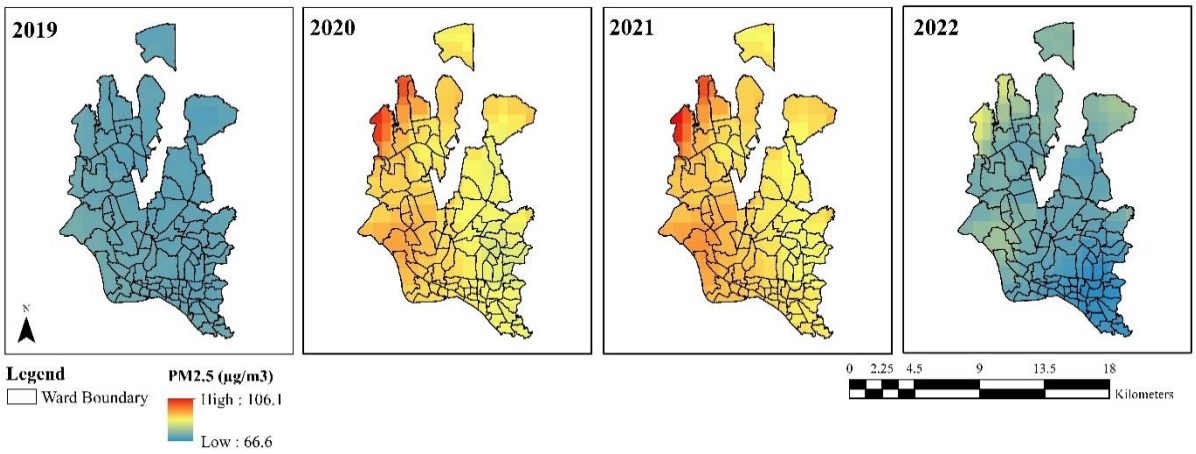

Figure 2 Annual mean $PM_{2.5}$ concentration distributions across the wards in Dhaka between 2019 and 2022 based on Global Annual $PM_{2.5}$ Grids at 0.01°×0.01° spatial resolution

The average NO_2 concentration over the six years from 2019 to 2024 was recorded at 208.21 µmol/m^2. Figure 3b and Figure 4 illustrate the highest concentrations in 2021 (257.42 µmol/m^2) and 2022 (264.54 µmol/m^2). In contrast, relatively lower concentrations were recorded in 2019 (183.99 µmol/m^2), 2020 (191.18 µmol/m^2), 2023 (193.37 µmol/m^2), and 2024 (158.76 µmol/m^2). In 2020, the world experienced a widespread lockdown due to the COVID-19 pandemic, which also took effect in Bangladesh. Between December 2019 and February 2020, the mean NO_2 concentration in Dhaka was recorded at 212.145 µmol/m^2. The first initial lockdown period lasted from March 26, 2020, to May 30, 2020 [82]. NO_2 levels fell to 120.80 µmol/m^2 in summer 2020 and further decreased to 67.12 µmol/m^2 in monsoon

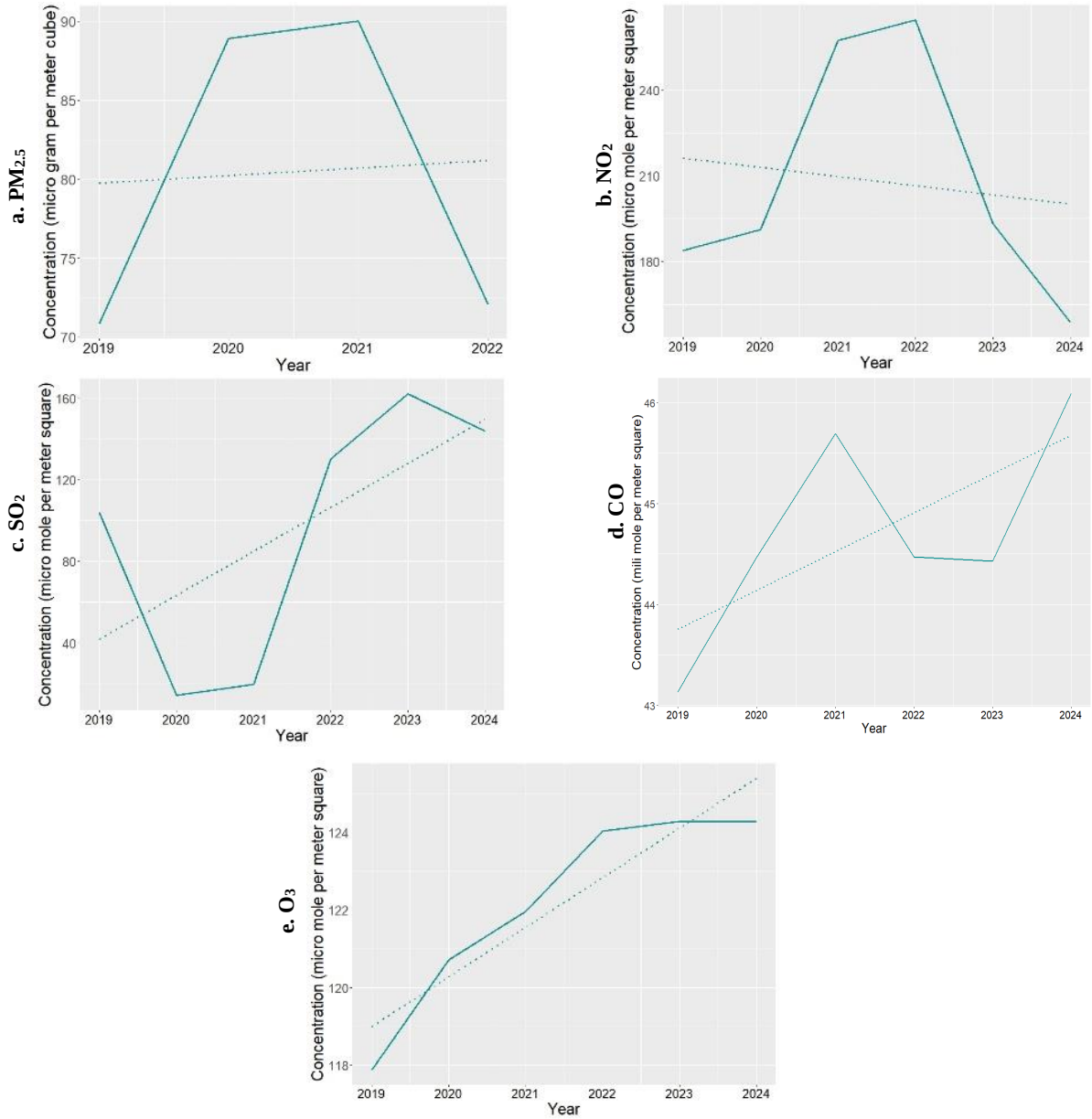

Figure 3 Annual changes of five criteria pollutants in the wards of Dhaka from 2019 to 2024: a. $PM_{2.5}$, b. NO_2, c. SO_2, d. CO, e. O_3

2020, representing decreases of 42.6% and 68.4%. Similar reductions were noted in Spain (Madrid) [83]; China [84]; Dhaka [44], [50]; and several cities in India such as Delhi [41], [50], [85]; Mumbai [41], [84]; Kolkata [41], [86]; Chennai [41]; and Hyderabad [41]. The diminished concentration levels in 2020 can be linked to the limitations placed on vehicular movement during the lockdown, corroborated by multiple studies [44], [83], [87], [88], [89]. NO_2 concentrations remained elevated post-2020, which could be attributed to inadequate enforcement of the lockdown protocols throughout 2021 [90]. Overall, the annual mean NO_2 concentration demonstrated a 13.71% reduction from 2019 to 2024, signifying a downward trend. While ascertaining the factors responsible for the decrease in NO_2 remains complex, it may relate to meteorological conditions, similar to the decline observed in $PM_{2.5}$ levels [81]. Notably, in 2024, NO_2 concentrations fell to the lowest levels recorded in six years, even dipping below those during the pandemic in 2020. Contributing factors could include a nationwide curfew mandated by the then Bangladeshi government following the student protests to abolish quotas in public sector employment, referred to as the Quota Reformation Movement. This curfew, in effect from July 20, 2024, curtailed educational activities and limited vehicular traffic [91], likely leading to the lower mean

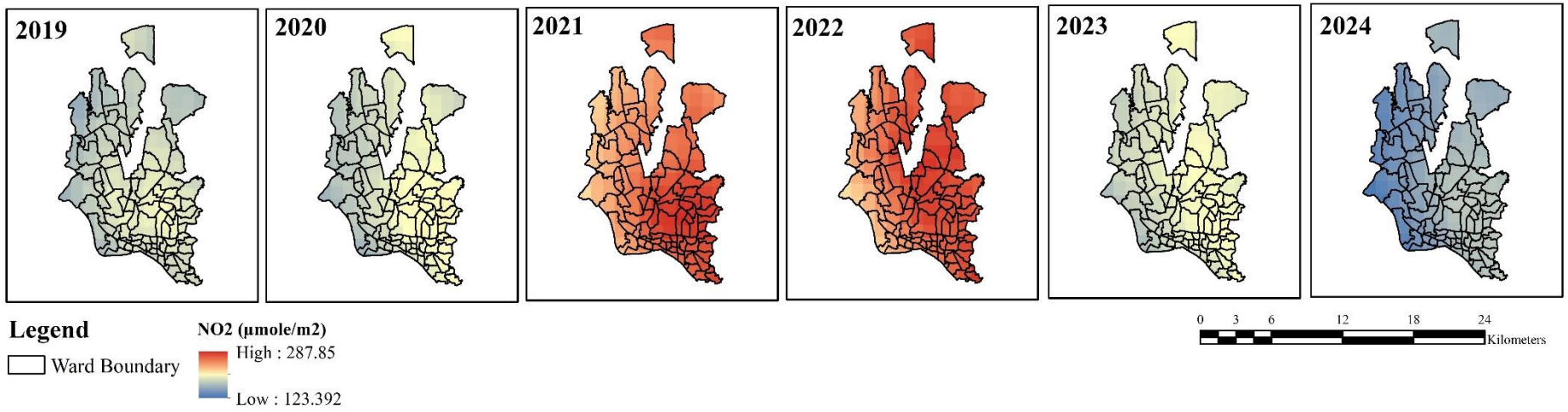

Figure 4 Annual mean NO_2 concentration distributions across the wards in Dhaka between 2019 and 2024 based on Sentinel 5P TROPOMI Sensors

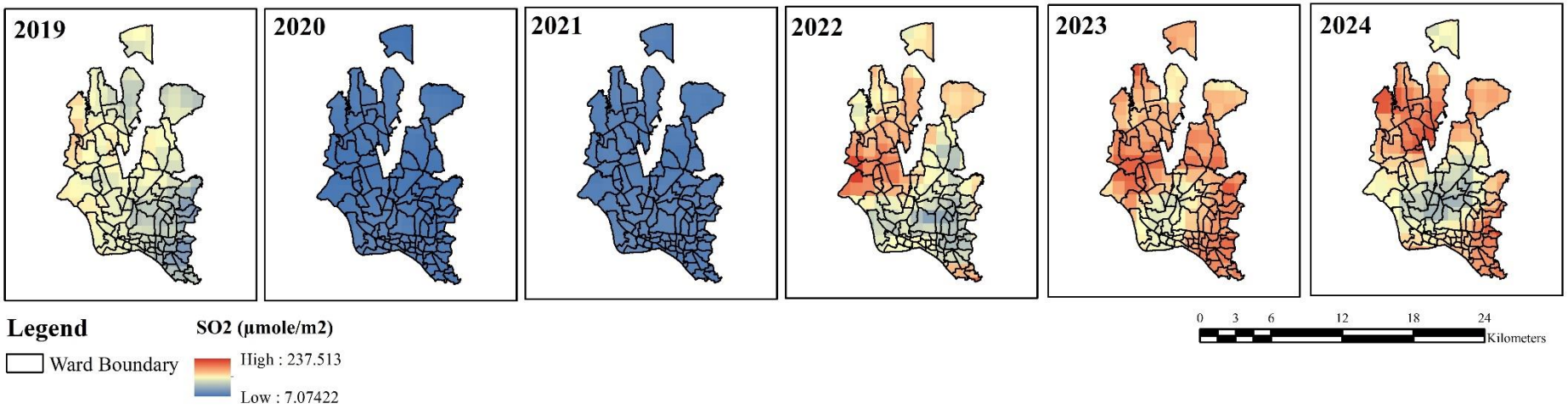

Figure 5 Annual mean SO_2 concentration distributions across the wards in Dhaka between 2019 and 2024 based on Sentinel 5P TROPOMI Sensors

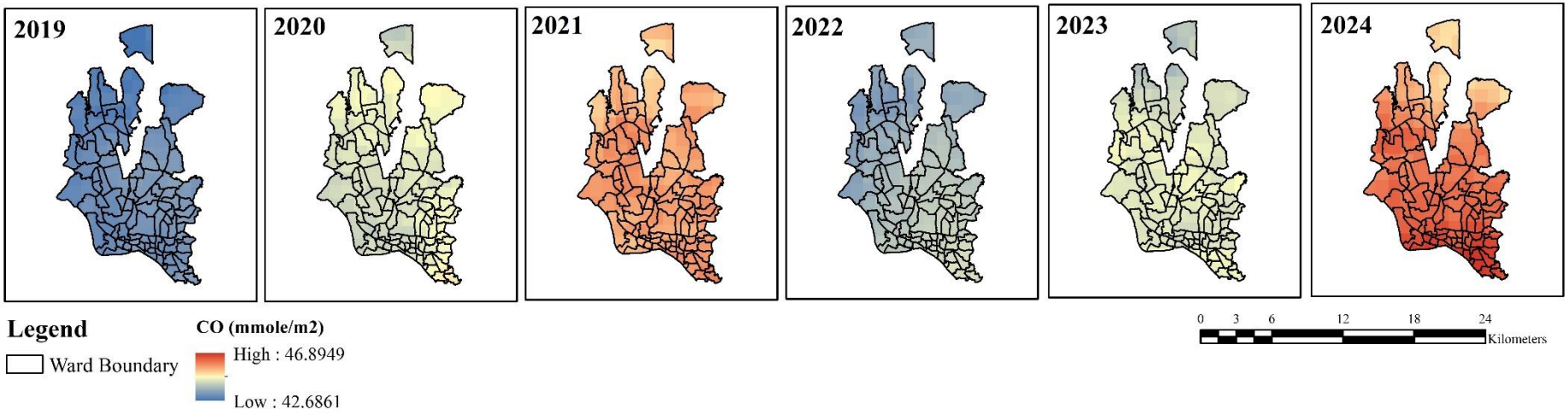

Figure 6 Annual mean CO concentration distributions across the wards in Dhaka between 2019 and 2024 based on Sentinel 5P TROPOMI Sensors

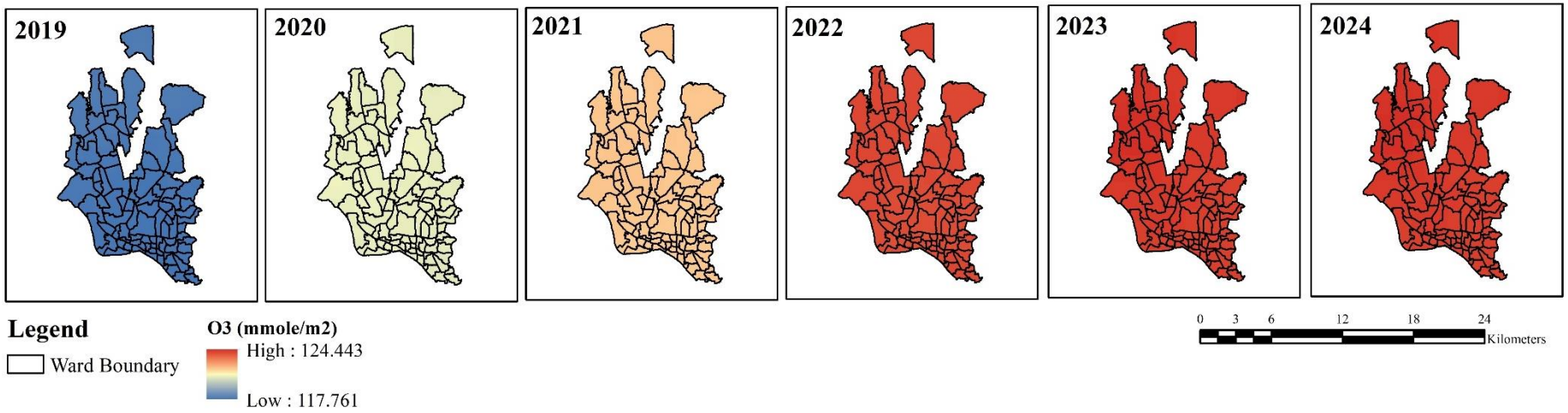

Figure 7 Annual mean O_3 concentration distributions across the wards in Dhaka between 2019 and 2024 based on Sentinel 5P TROPOMI Sensors

NO_2 concentration of 87.52 µmol/m^2 between June and September 2024.

The average concentration of SO_2 over the past six years stands at 95.66 µmol/m². A substantial increase of 38.53% in concentration between 2019 and 2024 suggests a rising trend in SO_2 pollution. However, Figure 3c and Figure 5 also revealed that SO_2 concentrations decreased and increased inconsistently, with a notable decline in 2020 and 2021. There was an 86.28% decrease in SO_2 levels in 2020 from 2019. Similar reductions in SO_2 levels have been recorded in China [91], [92], [93]; Italy [94]; several cities in India such as Delhi [41], [85]; Mumbai, Kolkata, Chennai, and Hyderabad [41]; and in eight major cities in Bangladesh [44]. After 2020, SO_2 levels rose marginally to 19.79 µmol/m^2 in 2021, although they remained relatively low. However, the concentration began to surge dramatically after 2021, reaching a peak of 162.05 µmol/m^2 in 2023 before slightly declining to 143.83 µmol/m^2 in 2024.

The average concentration of CO throughout the six years from 2019 to 2024 was noted at 44.71 mmol/m^2. Figure 3d and Figure 6 depict the variations in CO levels across the wards of Dhaka City during this period. The peak concentrations were recorded in 2024 (46.09 mmol/m^2), followed closely by 2021 (45.69 mmol/m^2). Concentrations were relatively lower in 2020, 2022 (44.47 mmol/m^2), and 2023 (44.43 mmol/m^2). The annual average CO concentration exhibited nearly a 6.86% increase from 2019 to 2024, indicating a rising trend overall.

The average O_3 concentration from 2019 to 2024 is 122.19 mmol/m^2. Throughout 2019 to 2024, a clear upward trend can be observed in the concentration of O_3, with an overall increase of 5% over six years, signifying growth in concentration. Figure 3e illustrates that ozone levels have risen almost linearly, reaching a peak mean concentration of 122.19 mmol/m^2 in 2024. Despite this upward trajectory, the change remains minimal across the area **(**Figure 7), maintaining a mean with a slight standard deviation of 0.03 mmol/m^2.

3.2 Seasonal Variation

A boxplot analysis was conducted to assess seasonal variations in pollutant concentrations, followed by the Kruskal-Wallis H test to determine statistically significant seasonal differences and a post hoc Mann-Whitney U test. Due to a lack of available data, a comprehensive seasonal analysis of $PM_{2.5}$ concentrations was not conducted. The findings are presented in Figure 8a-d and Table 3.

Table 3 reveals the median and Inter Quartile Range (IQR) values of the pollutants by season. For NO_2, winter demonstrated the highest median concentration (267.61 µmol/m^2). NO_2 pollution levels were higher, approximately 2.5 times in winter and 1.4 times in summer, compared to the monsoon. Regarding NO_2 spread, the IQR for NO_2 was widest in winter (29.09 µmol/m^2) and summer (25.78 µmol/m^2), indicating substantial variability, whereas the monsoon exhibited the least variability (Figure 8a). Previous studies have documented similar seasonal variations in NO_2 levels in India [21], [41], [50]; China [27], [28], [36]; and Bangladesh [13], [34], [38].

The median concentrations of SO_2 are significantly higher during the summer and winter compared to the monsoon season (Figure 8b), with pollution levels being approximately 40.5 times greater in these periods. The wide dispersion of SO_2 in winter and summer is also apparent, with an IQR of 44.27 µmol/m^2 in winter and 37.79 µmol/m^2 in summer versus a narrower distribution during the monsoon (IQR of about 12 µmol/m^2). Numerous studies in India [21], [41]; China [28], [28]; and Bangladesh [13] have consistently shown that SO_2 pollution peaks in winter and reaches its lowest levels during the monsoon. While the median concentration of CO in winter surpasses that of both summer and monsoon (Figure 8c), the variability in concentration remains relatively uniform across all three seasons, as evidenced by the low IQR values for CO across each season. Seasonal variations in CO with maximum concentrations in the winter are also observed in Kuwait [95]; China [27], [28]; India [41], [96]; and Bangladesh [13], [40].

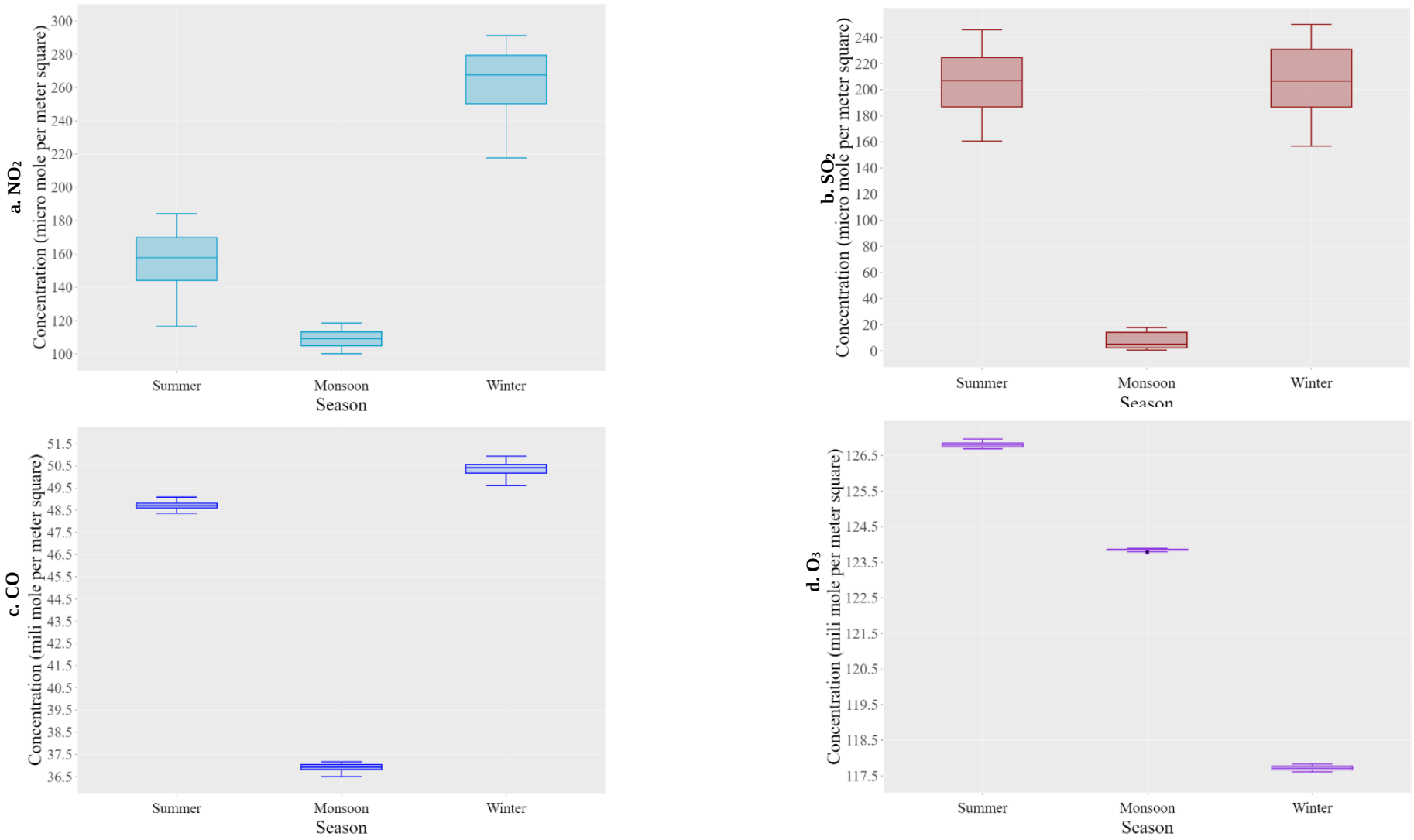

Figure 8 Box whisker plots for seasonal pollution variation across the wards in Dhaka averaged over six years between 2019 and 2024; a. NO_2, b. SO_2, c. CO, d. O_3. Seasons are categorized as follows: summer (March-May), monsoon (June-September), and winter (December-February)

The Kruskal-Wallis H test revealed significant seasonal NO_2, SO_2, and CO variations. The tests yielded χ^2 values of 390133, 296540, and 230821, respectively, with all p values being less than 2.2×10^{-16}, rejecting the null hypothesis. Follow-up post-hoc Mann-Whitney U tests performed for NO_2, SO_2, and CO demonstrated that pollution levels were significantly elevated in winter compared to the monsoon and summer ($p < 2\times 10^{-16}$), with summer also exhibiting a considerable difference from monsoon ($p < 2\times 10^{-16}$).

In contrast to other pollutants, O_3 displayed a unique seasonal trend, with the peak median concentration occurring in summer, followed by monsoon, while winter recorded the lowest concentration (Figure 8d). Other studies also reflect this reversal trend [27], [42]. The dispersion of O_3 data was narrow, with monsoon exhibiting the least variability (IQR = 0.03 mmol/m²). The Kruskal-Wallis H test verified significant seasonal differences (χ^2 (2) = 390144, $p < 2.2 \times 10^{-16}$), and post-hoc analysis indicated that summer O_3 levels were significantly higher compared to those in monsoon and winter ($p < 2 \times 10^{-16}$).

Table 3 Seasonal variation of pollutants' concentrations (NO_2, SO_2, CO, and O_3) across summer (March-May), monsoon (June-September), and winter (December-February) between 2019 and 2024

		Summer	**Monsoon**	**Winter**
NO_2 (µmol/m^2)	Max	184.19	118.55	291.21
	Q_3	169.92	113.17	279.32
	Median	157.84	109.09	267.61
	Q_1	144.10	141.91	250.23
	Min	116.56	100.05	217.68
	IQR	25.82	8.26	29.09
SO_2 (µmol/m^2)	Max	245.78	17.79	249.93
	Q_3	224.58	14.11	230.96
	Median	206.83	5.10	206.65
	Q_1	186.79	2.25	186.69
	Min	160.48	0.51	156.77
	IQR	37.79	11.86	44.27
CO (mmol/m^2)	Max	49.09	37.17	50.93
	Q_3	48.81	37.04	50.57
	Median	48.70	36.92	50.41
	Q_1	46.61	36.82	50.17
	Min	48.36	36.50	49.61
	IQR	0.20	0.22	0.40
O_3 (mmol/m^2)	Max	126.97	123.90	117.83
	Q_3	126.86	123.87	117.77
	Median	126.80	123.86	117.71
	Q_1	126.74	123.84	117.66
	Min	126.69	123.78	117.61
	IQR	0.12	0.03	0.11

3.3 Spatial Distribution of Pollutant Concentrations

$PM_{2.5}$ levels in all wards of Dhaka exceed both national and international guidelines. However, the pollution appears to be more concentrated in certain wards of the city. The spatial distribution of average $PM_{2.5}$ concentration in the wards of Dhaka from 2019 to 2022 is shown in Figure 9. Primarily, $PM_{2.5}$ accumulation is observed in wards located in the west of the city. Figure 11a illustrates that while $PM_{2.5}$ is notably dense in the western wards, a comparison reveals that particulate pollution is substantially higher in the wards of DNCC than DSCC. The figure indicates that wards within DNCC-Zone 5 (ward

26, 27, 28, 29, 30, 31, 32, 33, 34), DSCC-Zone 1 (ward 15, 16, 17, 18, 19, 20, 21), DNCC-Zone 3 (ward 18, 19, 20, 21, 22, 23, 24, 25, 35, 36), DNCC-Zone 4 (ward 9, 10, 11, 12, 13, 14, 16), and DNCC-Zone 2 (2, 3, 4, 5, 6, 7, 8, 15) exhibit $PM_{2.5}$ levels around or exceeding 80 µg/m^3, which is eight times higher than the WHO recommendations and five times above the BNAAQS standards. These areas encompass some of the most important and busy parts of Dhaka, including Adabar, Mohammadpur, Lalmatia, Shyamoli, Sher-e-Bangla Nagar, Asadgate, Khamarbari, Farmgate, Bijoy Saroni, Dhanmondi, Kathal Bagan, Kolabagan, Dhaka College and Newmarket area, Mouchak, Ramna Park, Dhaka University Area, Eastern Pallabi, Shewrapara, Kazipara, and Mirpur (1, 2, 10, 11¸ 12,13,14). Specific wards, such as wards 6, 8, 33, and 34 in the north and wards 14 in the south, face particulate pollution levels exceeding 85 µg/m^3, indicating hazardous pollution levels. These wards include Mirpur 1, Eastern Pallabi, Mohammadpur, Lalmatia, and Hazaribag. Furthermore, DSCC Zone 3 and Zone 5, which cover Lalbag, Azimpur, Islam Bag, Kamrangichar, Chawkbazar, Wari, Jatrabari, Gandaria, Sayedabad, Shyampur, and Jurain, are also experiencing elevated $PM_{2.5}$ levels.

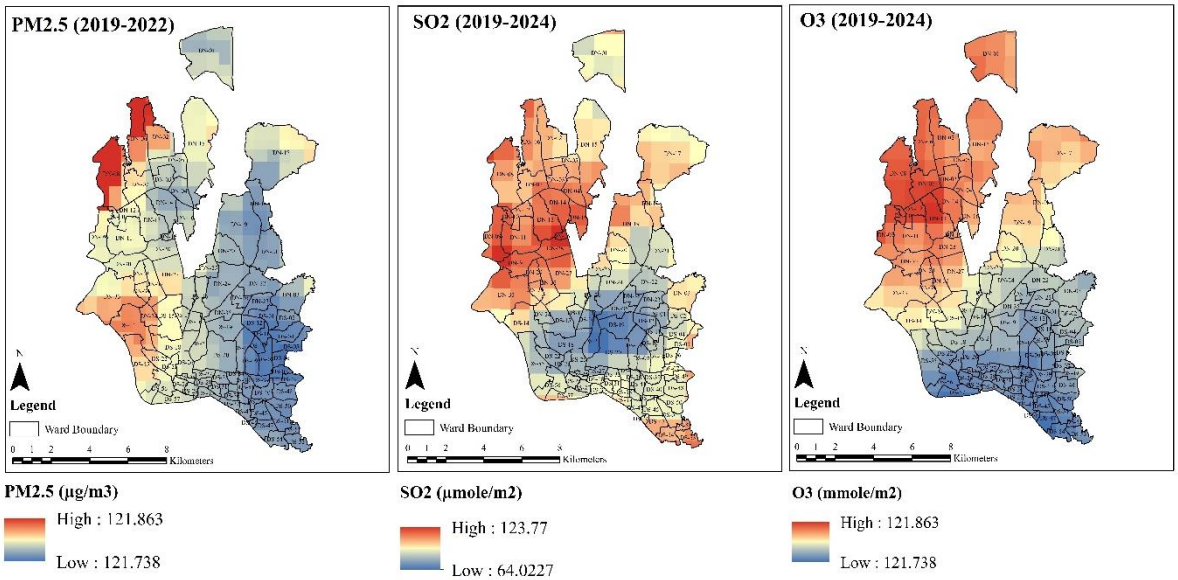

Figure 9 Spatial distributions of annual concentrations of $PM_{2.5}$, SO_2, and O_3 averaged from 2019 to 2024 across the wards of Dhaka

The spatial distribution of SO_2 reveals higher concentrations in the wards situated to the west, while lower levels are shown in the eastern wards, as illustrated in Figure 9. Wards within DNCC zones that recorded elevated $PM_{2.5}$ levels also exhibit increased SO_2 concentrations, and similar to $PM_{2.5}$, SO_2 pollution is more pronounced in DNCC than DSCC, as demonstrated by Figure 11b. In DSCC Zone 5, which includes wards 47, 52, 53, 54, 56, and 57, substantial SO_2 clusters are represented by shades of red. These regions encompass Shyampur and Gandaria in southern Dhaka. Regarding O_3, the spatial distribution pattern of O_3 is marked by heightened concentrations in the northwestern wards, which gradually diminish towards the southeast (Figure 9). However, the distribution has remained relatively consistent across all wards, evidenced by a standard deviation of 0.03 mmol/m^2.

In contrast, the spatial distribution of NO_2 shows a contrasting trend from that of $PM_{2.5}$, SO_2, and O_3. NO_2 is primarily concentrated in the eastern wards of DSCC and DNCC, with NO_2 pollution values declining progressively from east to west (Figure 10). In Figure 10, clusters highlighted in red and orange represent elevated NO_2 levels, predominantly found in the DSCC wards, indicating a greater concentration of NO_2 in south Dhaka compared to the north. This observation is further validated by the bar charts in Figure 11c, which illustrate that all DSCC Zones 1-5 face higher levels of NO_2 pollution than their DNCC wards. The highest concentrations of NO_2 are experienced in DSCC Zone-2

(1,2,3,4,5,6,8,9,10,11,12,13), which includes areas such as Khilgaon, Goran, Aftabnagar, Basabo, Razarbag, Mugdapara, Komlapur, Motijheel, Malibagh Bazar Road, Chameli Bag, and Rajarbag Police Line Area. Following this are DSCC Zone 1 (15,16,17,18,19,20,21), DSCC Zone 4 (30,31,32,33,34,35,36,37,38,42,43), and DSCC Zone 5 (7,39,40,41,44,45,46,47,48,49,50,51,52,53,54). These zones encompass regions like Dhanmondi, Kathalbagan, Dhaka College and New Market area, Mouchak, High Court and Dhaka University Area, Chawkbazar, Bongshal, Nazira Bazar, Kotwali, Wari, Shyampur, Jatrbari, Dhupkhola, and Gandaria areas of the DSCC. Substantial concentrations of NO_2 can also be observed in DNCC wards within Zones 1, 2, and 3. These wards are in Uttara Sectors 1, 4, 11, Mirpur 1, 2, 7, 11, 12, 13, 14, Tejgaon, Khilgaon, Rampura, Gulshan, and Badda. Among the city corporation zones, DNCC Zone-5 exhibits relatively lower NO_2 pollution levels, which includes areas such as Mohammadpur, Asad Gate, Adabar, Shyamoli, Farmgate, and Bijoy Saroni.

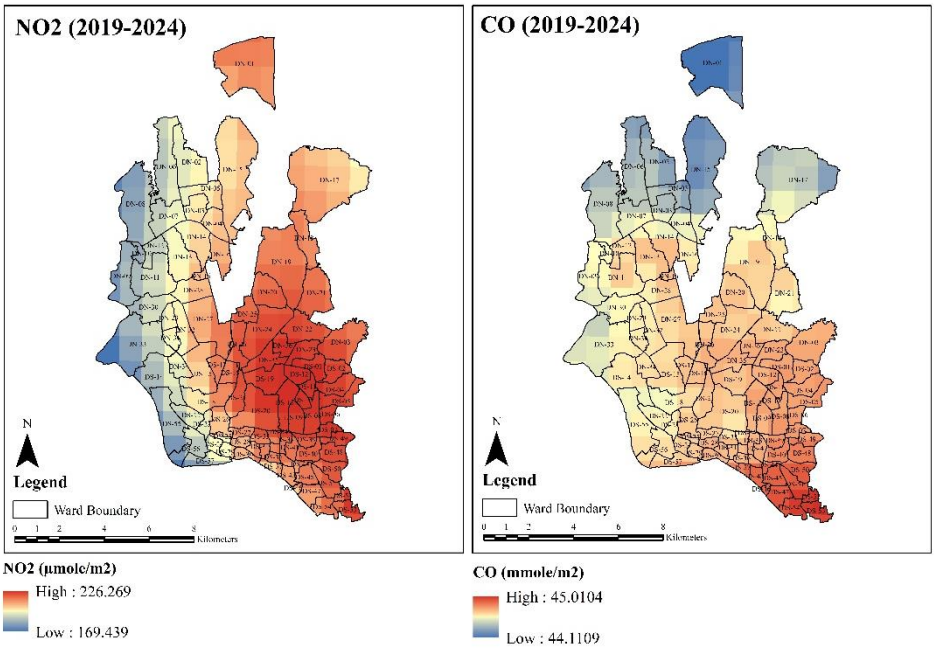

Figure 10 Spatial distributions of annual concentrations of NO_2 and CO averaged from 2019 to 2024 across the wards of Dhaka

The spatial distribution of CO reveals heightened concentrations in the southeast, with lower values notably present in the northwestern wards (Figure 10). This trend is similar to NO_2, with elevated levels observed in the wards of DSCC compared to those of DNCC. Higher CO concentrations can be detected in DSCC Zones 2, 3, 4, and 5, while the lowest levels are found in DNCC Zones 4 and 5 (Figure 11d). However, the spatial distribution of CO throughout the study area has remained relatively uniform, showing a standard deviation of 0.17 mmol/m^2, indicating that the mean concentration across the wards is closely aligned and has not fluctuated substantially.

3.4 Environmentally Critical Area Analysis

A deductive indexing method was employed to assess the impact of air pollutants across various wards, leading to the identification of environmentally critical areas. Index generated from critical area ranking ranges from 0 to 1, with values close to 0, indicating low vegetation and high pollutant levels, to values near 1, which denote high vegetation coverage and reduced air pollution. Based on the index values, the wards were categorised as lightly degraded, moderately degraded, and highly degraded areas. The results are shown in Table 4 and Figure 12.

Table 4 Land use distribution by degradation level derived based on vegetation coverage and cumulative concentration of air pollutants ($PM_{2.5}$, NO_2, SO_2, CO, and O_3) between 2019 and 2022

	Area (in acres)			
Land Use	**Lightly Degraded**	**Moderately Degraded**	**Highly Degraded**	**Grand Total**
Administrative	185.24	138.16	80.03	**403.43**
Agriculture	73.60	21.04	1.17	**95.81**
Commercial	440.74	798.76	750.99	**1990.49**
Community Facilities	80.81	399.98	171.38	**652.17**
Education and Research	1016.95	867.41	297.03	**2181.39**
Health Facilities	196.35	73.31	29.58	**299.24**
Industrial	107.27	512.24	215.22	**834.73**
Institutional	354.19	382.82	24.23	**761.24**
Mixed Use	580.07	2085.13	2421.34	**5086.54**
Open Space	1318.18	282.86	110.21	**1711.25**
Residential	4884.16	8313.57	4732.40	**17930.13**
Restricted	1957.41	942.88	209.98	**3110.27**
Transport and Communication	1,041,168.22	9,42,764.47	1,093,593.04	**30,77,525.73**
Vacant Land	1089.06	1154.13	143.82	**2387.01**
Grand Total	**10,53,452.25**	**9,58,736.75**	**11,02,780.41**	**31,14,969.42**

Table 4 illustrates the allocation of various land use categories (in acres) across distinct levels of degradation: Lightly Degraded, Moderately Degraded, and Highly Degraded. It indicates that most regions are highly degraded in terms of area coverage. Highly and moderately degraded areas generally exhibit a greater prevalence of transport, residential, mixed land uses, and commercial activities. In contrast, lightly degraded areas are characterised by a higher proportion of agriculture, open space, health facilities, and administrative land use. It is also noteworthy that transport stands out as the primary land category contributing to land degradation, followed by residential and mixed-use areas.

The overall environmental quality is illustrated in Figure 12 by assessing the vegetation coverage (NDVI) alongside air pollutants ($PM_{2.5}$, NO_2, SO_2, CO, and O_3) averaged over four years. The index values across the wards varied from 0.16 to 0.55, suggesting that all wards exhibit low vegetation coverage and elevated levels of air pollutants. The red clusters depicted on the maps represent areas substantially degraded due to minimal vegetation cover and high concentrations of contaminants. The severely impacted wards include Ward-5 (DNCC Zone 2); 12, 13, 14 (DNCC Zone 4); 29, 30, 34 (DNCC Zone 5); and in the DSCC wards 12, 13 (DSCC Zone 2); 22, 23, 24, 25, 28, 29 (DSCC Zone 3); 30-38, 41, 42 (DSCC Zone 4); 45, 47, 48, 51, 52, 53, 54 (DSCC Zone 5). Prominent among these degraded areas are Mirpur-11, Kazipara, Mohammadpur, Shamoli Ring Road, Malibagh Bazar Road, Razarbag, Purana Paltan, Hazaribagh, New Paltan Lane, Lalbagh Durg Road, Shaista Khan Road, Chawkbazar, Kotwali, Bangshal, Gandaria, Saidabad, Jatrabari, Dholai Para, and Jurine. Upon closer examination of the spatial distribution, it is evident that most wards within the study area are moderately degraded. These wards are dispersed throughout the city. Similarly, due to a relatively higher presence

of green spaces and lower concentrations of pollutants, a few wards experience a low pollution level. These wards are mainly in the northern and middle parts of the city, with only one ward in the southern part. The wards in the southern part of the city are highly degraded due to a lack of green space.

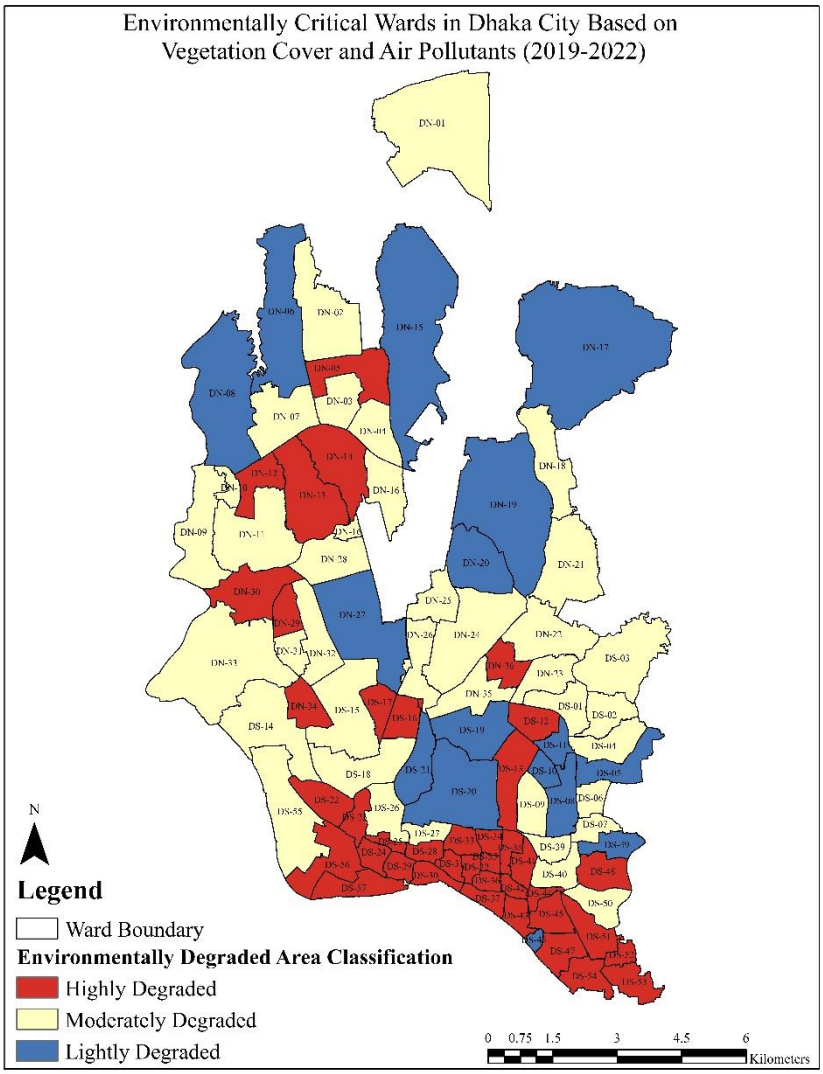

Figure 12 Environmentally critical Dhaka North and South City Corporations classification based on vegetation coverage (NDVI) and air pollutants ($PM_{2.5}$, NO_2, SO_2, CO, and O_3)

4. Discussion

The air pollution and air quality analysis in Dhaka from 2019 to 2024 reveals a concerning upward trend in the annual mean concentrations of pollutants, except NO_2. Notably, $PM_{2.5}$ levels increased by 1.72%, SO_2 by 38.58%, CO by 6.86%, and O_3 by 5.44%, highlighting a deterioration in air quality across the wards of the city. Statistical evidence of such an increasing trend in air pollution levels has also been reported by [13], [97]. Despite the most modest increase amongst the five pollutants, $PM_{2.5}$ continues to represent the most hazardous pollutant across the wards of Dhaka, frequently exceeding national and international safety standards from 2019 to 2022. Various factors contribute to these rising levels, including transportation, industrial activities [98], [99], cooking, heating, and construction [28], [101], compounded by adverse meteorological conditions [43], [101]. Dust pollution, exacerbated by ongoing infrastructure projects like the Dhaka Metrorail and the Elevated Expressway, raised the risk of dust contamination by a factor of many [97]. 7.70% of road dust and 7.57% of soil dust contribute to $PM_{2.5}$ levels in Dhaka city [42]. Furthermore, in Bangladesh, particularly within megacities such as

Dhaka, approximately 35% of ambient PM_{10} and approximately 15% of $PM_{2.5}$ are produced by emissions from brick kilns and transportation systems [102]. The primary source of increased SO_2 concentrations is also linked to brick kiln emissions [13], [97]. Meanwhile, despite a declining trend attributable to meteorological factors and political unrest, NO_2 concentrations remain a considerable concern for Dhaka. The predominant source of NO_2 and CO pollution in densely populated regions such as Dhaka is frequently ascribed to vehicular [13]. A regional air quality report indicates that the rising NO_2 levels result from heavy reliance on fossil fuels, expanded industrial activities, and a growing number of vehicles over the preceding decade [103], with over 5.983 million registered motor vehicles as of January 2024 [104]. Many of these vehicles are outdated and inadequately maintained, exacerbating the increasing concentrations of NO_2 [103]. The current trajectory of vehicle growth, paired with inadequate technology and traffic management, poses a potential risk for future NO_2 levels in Dhaka [105]. The Centre for Atmospheric Studies (CAPS) chairman stated that pollution from these sources could have been averted if the City Corporation, the Ministry of Local Government, and the Department of Environment (DoE) had collaborated effectively. China, a nation facing air quality challenges similar to those of Dhaka, has been prosperous in reducing emissions of $PM_{2.5}$, PM_{10}, SO_2, NO_2, and CO [27], [28], [40], resulting from the implementation of multifaceted actions, including adaptation of Air Pollution Action Plan [27] and Coal Cap policies [107]. The Bangladeshi government also has comparable policy initiatives, with some success with the rollout of the Brick Kiln Control Act 2013 [33], contributing to decreased $PM_{2.5}$ levels between 2014 and 2017 [31]. However, the recent rise in $PM_{2.5}$ and SO_2 concentrations indicates inadequate policy enforcement. Numerous brick kilns on the outskirts of Dhaka continue to operate outside legal parameters.

Although there was a general rise in air pollution from 2019 to 2024, the study indicated an improvement in air quality during 2020. In Bangladesh, the first nationwide lockdown was announced on March 26, 2020, and it remained in effect until May 31, 2020. The comparative study showed that the levels of NO_2, SO_2, and CO during the lockdown period from March to May 2020 decreased by 42.59%, 7.12%, and 2.50%, respectively, compared to the period before the lockdown (December-2019-February 2020). This decline in pollution levels can be linked to the halt of industrial operations in Dhaka and restrictions on vehicle movement throughout the 2020 lockdown [41], [43], [44]. Conversely, O_3 levels rose during the same timeframe, as corroborated by various other studies [41], [43], [44]. It is essential to consider weather patterns, emissions, and regional air quality conditions that can influence the increase in O_3 concentration [41]. The lack of $PM_{2.5}$ data prevented a comprehensive analysis of its levels during the lockdown. However, the global pandemic persisted for over two years, and despite the restrictions on movement and a second lockdown in April 2021, each pollutant's concentrations peaked in 2021. This suggests a lack of effective control over the lockdown and restriction measures [90], returning to pre-pandemic emission levels and economic activity [41].

The results also suggest that levels of NO_2, SO_2, and CO pollution are significantly higher during the winter months (December-February), followed by the summer (March-May) and monsoon (June-September). Key factors influencing these variations include weather conditions [107], the operation of brick industries between November and June, the long-range transport of fine particles, and low atmospheric diffusion in winter, which contribute to elevated pollution levels [13], [27]. In contrast, the monsoon season sees reduced pollution, attributed to increased wind speeds and precipitation that wash away dust particles [13], [21]. Similar seasonal patterns have been identified in studies conducted in China [27], [28], [36]; Delhi [50], [108], Kolkata [109]; Agra [110]; and Dhaka [13], [38], [50]. Concerning variability, SO_2 and NO_2 had the widest dispersion and larger variation between winter and monsoon, as well as between summer and monsoon pollution levels, while CO and O_3 displayed the least variability, similar to the findings of [50]. Since rain disrupts the processes of brick making, drying,

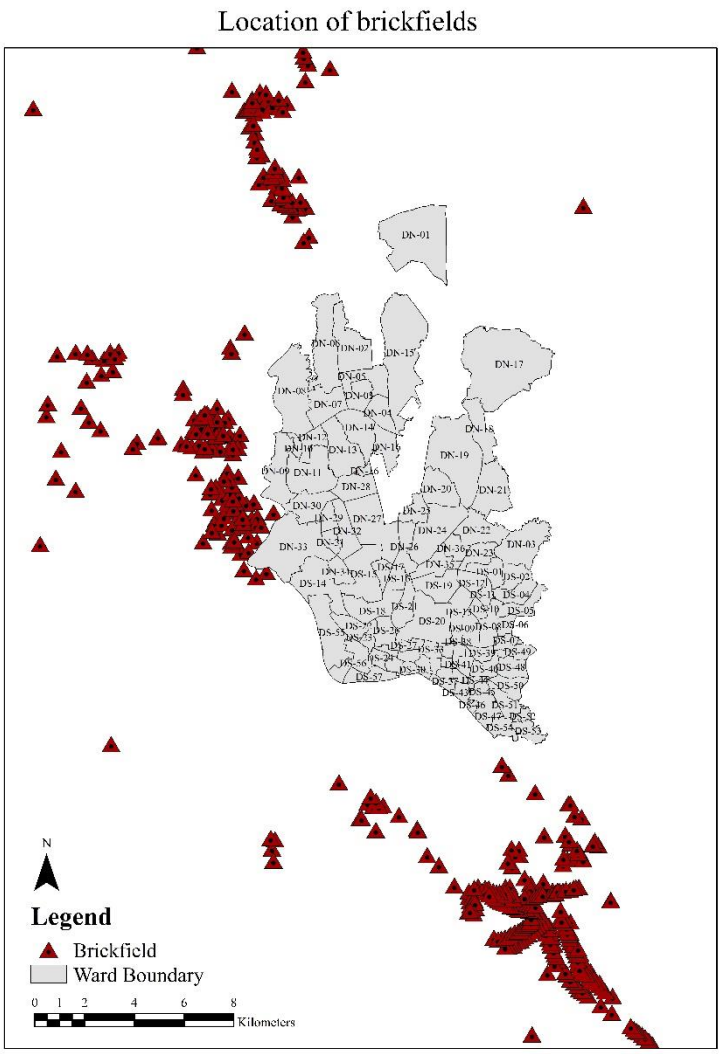

Figure 13 Location of brickfields around Dhaka City

and firing, brick production is primarily conducted from November to June [111], which indicates a widely fluctuating spatial concentration of SO_2. On a different note, O_3 displays an inverse seasonal trend, peaking in summer due to heightened heat and sunlight promoting vigorous photochemical reactions involving NO_x and volatile organic compounds (VOC) [27]. O_3 levels are moderate during the monsoon and the lowest readings in winter. The reduced solar radiation in winter increases the chances of air pollution events like smog and haze, leading to diminished air visibility and a decrease in ultraviolet radiation [27].

Regarding the spatial distribution of pollutant concentrations, $PM_{2.5}$, SO_2, and O_3 display a comparable trend, while CO and NO_2 follow a distinct pattern separate from the first three pollutants, findings similar to [41]. The observed spatial concentrations can be linked to the proximity to sources of emissions. The distributions of SO_2 and O_3 are similar, revealing a low concentration in the southwest and a higher concentration towards the northwest. The primary observation is that regions in these wards face elevated levels of SO_2 pollution due to their proximity to brick manufacturing industries. Figure 13 shows that brickfields surrounding Dhaka are located near the city corporation wards in the west, particularly in the vicinity of DNCC zones 2, 4, 6, and DSCC zone 6. Additionally, heavy diesel-fueled vehicles contribute to the SO_2 emissions as they transport garment products [112] from surrounding textile industrial clusters located in Savar, Ashulia, Tongi, Tejgaon, Old Dhaka, and Narayanganj, all in proximity to high SO_2 emission zones. Similarly, $PM_{2.5}$ concentrations are notably higher in the

western wards, mirroring the spatial trend seen with SO_2. In addition to brick industries raising $PM_{2.5}$ levels, various infrastructure projects are underway in these wards under the DNCC. Major initiatives such as the Dhaka MRT, BRT, and Elevated Expressway are being developed in these areas. According to the findings, elevated NO_2 levels are primarily found in the eastern wards of both DSCC and DNCC, showing a spatial distribution contrary to $PM_{2.5}$ and SO_2, with NO_2 values diminishing gradually from east to west. These areas encompass one of the study region's most congested road networks. Figure 14 illustrates the locations of CNG filling stations, bus stops and terminals, boat ghats, train stations, ferry terminals, toll booths, and truck terminals. These transportation hubs are located in regions where NO_2 levels are elevated. Besides, the spatial pattern of CO aligns with that of NO_2, with high concentrations in the east and lower concentrations in the west of DSCC and DNCC. A similar spatial trend between CO and NO_2 was observed in another study [46], attributing it to Dhaka's primary source of vehicular emissions [13].

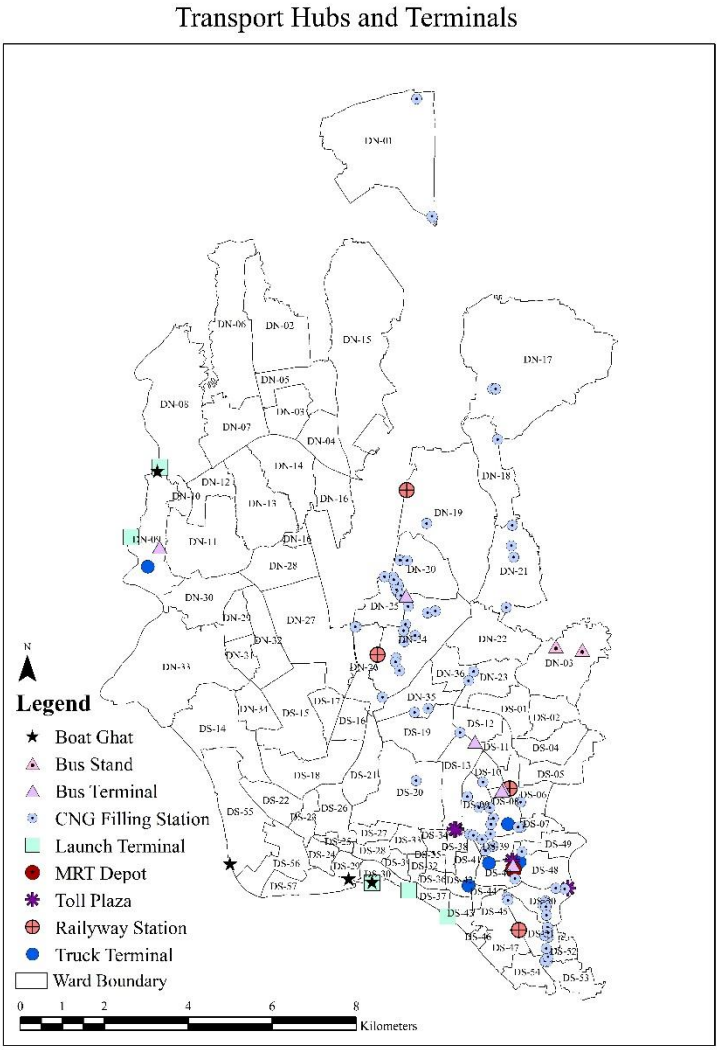

Figure 14 Location of boat ghat, bus stand, bus terminal, CNG filling station, launch terminal, MRT depot, toll plaza, railway station, and truck terminal in the study area

Environmentally critical area analysis revealed three clusters of deteriorated areas based on vegetation coverage and air pollution. The most severely affected clusters are in Old Dhaka. Wards in the southern part of the city, particularly Old Town, experience elevated levels of air pollution despite having less exposure to vehicular emissions than other wards. The study indicates that environmental conditions are better with agriculture, open spaces, and health facilities, while transportation and commercial

activities contribute to deterioration. Old Dhaka's severe degradation could be linked to dense residential structures and industrial land use, with areas having less than one per cent dense vegetation coverage [113]. The moderately polluted zones primarily represent the commercial and industrial core of the city. Motijheel is the commercial hub, while Tejgaon and Hazaribag are designated industrial areas. These locations are characterised by the city's most active road and rail networks, which are marked by substantial motor vehicle traffic and fuel combustion. Peripheral areas such as Mirpur-11, Uttara, Gabtoli, and Technical are situated near brickfields and act as gateways to enter Dhaka, with heavy traffic flowing through them regularly. In this sense, it supports the study's results that environmental quality will decline as commercial and transportation land uses spread. In the study region, Mirpur-1 (Zoo and Botanical Garden), Vasantek, Kuril, Khilkhet, Gulshan Banani, Niketan, Monipuripara, Kadamtala Basabo, Gopibagh, Motijheel Colony, Shahjahanpur Railway Colony, Mintu Road, Kakrail, Siddeshwari, Topkhana Road, Dhaka University area, and Dhalpur are areas with lightly degraded conditions, possibly due to encompassing relatively more green spaces and water bodies.

5. Policy Implications

The spatio-temporal variation trend of air pollutants offers a scientific foundation for spatially targeted pollution control policies in Dhaka. Air pollution can indeed be mitigated through well-crafted policies, as evidenced by the successful reduction of pollution in China from 2014 to 2019 [24], [28]. The government of Bangladesh also made progress in lowering $PM_{2.5}$ levels in Dhaka for two years [43], but later struggled to sustain these improvements due to weak policy enforcement. The rising air pollution observed over the past six years underscores the urgent need for strict regulations on air pollution patterns through policies. The current regulatory laws, including several acts and the newly introduced Air Pollution Control Rules 2022, address various strategies considering socio-economic structures, topographical characteristics, meteorological variations, and existing pollution sources [114], which is commendable. However, the national air quality standards in Bangladesh do not account for land use criteria such as residential, industrial, and environmentally sensitive areas when setting air quality standards. The current research indicates a close relationship between environmental quality and land use, with the most degraded areas typically found in residential, mixed, commercial and transport hubs. In contrast, Indian standards effectively integrate land use categories, including residential, industrial, and environmentally sensitive areas [115], suggesting that Bangladesh could benefit from adopting a similar approach to regulate standard limits at the land use level. The research also revealed that air pollution considerably intensifies during the winter and summer. Therefore, it is crucial to develop seasonal mitigation strategies with increased frequency of water sprinkling, construction control, and brick kiln monitoring, especially in wards with low vegetation. The Air Pollution Control Rules 2022 mandate the application of dust-controlling chemicals in polluted areas at least twice. While the DNCC and DSCC have initiated water sprinkling during winter pollution events, these measures have been largely ineffective.

Air pollution in Dhaka arises from various pollutants distributed across wards, necessitating ward-specific management strategies. There is an uneven distribution of the sources of air pollution. For instance, emissions from construction and brick kiln sites are concentrated in the city's outer west, whereas vehicle exhaust emissions are more concentrated on roadways, core commercial districts, and transportation terminals. As a result, the city-scale action plan is failing to reduce the level of air pollution at the urban hotspot. To lower the pollution level in a designated area, the city must implement a location-specific air quality management strategy [116], [117]. Per the Air Control Rules 2022, the government can designate an area as a 'Degraded Airshed' if it consistently exceeds permissible air quality limits, limiting new industrial or settlement developments and relocating existing pollution sources. The study mapped the spatial distribution of individual pollutants. It identified cumulatively

polluted, degraded areas, enabling residents to evaluate the degraded air mapping for their specific area, allowing those with respiratory conditions to select a safer living environment. This analysis could be aligned with the Air Pollution Control Rules 2022 in identifying degraded air sheds and highlights the essential roles of local authorities, such as the Dhaka North and South City Corporations, in managing air pollution. Recently, DNCC and DSCC have developed separate Climate Action Plans in conjunction with the National Adaptation Plan (2030-2050) for their respective administrative areas. However, air quality was not included in the vulnerability assessments of wards in these Climate Action Plans. Therefore, it is recommended that both city corporations incorporate air quality measures within their strategies, similar to the critical area ranking presented in the current study, to pinpoint environmentally degraded air pollution areas and evaluate the vulnerable wards across Dhaka.

6. Conclusion

Dhaka is experiencing significant urbanisation challenges, including traffic congestion, poor road conditions, and increasing air pollution due to industrial emissions, imposing greater pressure on local authorities, decision-makers, and relevant stakeholders. This research analyses air pollutants from 2019 to 2024 to assess the spatial and temporal dynamics of atmospheric pollution across the city's wards. The study has enhanced the existing understanding of air pollution in Dhaka by considering NO_2, SO_2, CO, and O_3 in addition to $PM_{2.5}$. Results highlight that $PM_{2.5}$ exceeds recommended safety standards across all wards, while other pollutants such as NO_2, SO_2, CO, and O_3 show an upward trend. Although these pollutants may currently remain within the standard limits, such an increasing trend could pose serious hazards in the foreseeable future. Besides, ward-wise information on air pollution would benefit urban planners and decision-makers in effectively managing air quality in Dhaka. The analysis reveals ward-wise spatial variability in pollutant concentrations, with higher $PM_{2.5}$, SO_2, and O_3 levels found in the western wards linked to brick industries and construction. In contrast, the eastern wards experience greater NO_2 and CO levels due to dense transportation networks. Again, rather than only assessing the individual effects of each pollutant, the research collectively identifies the wards most impacted by air pollution. It shows that wards with high transportation, residential, mixed, and commercial use suffer considerable degradation, while those with more greenery and water bodies experience lesser effects. These insights can aid decision-makers in formulating effective strategies for enhancing air quality in the affected wards.

The study examines air pollutant levels derived from satellite remote-sensing imagery, which can be contrasted with estimates of near-surface pollutant concentrations. Although the results are meaningful and practically relevant for Dhaka city, verifying the data through in situ measurements is essential for future research. However, the limited number of ground monitoring stations hinders accurate representation of local air pollution patterns, underscoring the need to enhance these networks. Further analysis of spatial interpolation methods for remote sensing is necessary, particularly in urban settings where observation stations are infrequently situated. Air pollutants demonstrate variations across seasons, times of day, and days of the week; additionally, the impacts of meteorological factors, long-range transport, and pollutant transformation have yet to be thoroughly investigated. Future research focusing on the wards of Dhaka should seek to assess these influences to gain insights into how physical and chemical factors affect air pollutant concentrations across the wards.

Funding

No funding was received for this work.

CRediT Authorship Contribution Statement

This manuscript is original, has not been published before and is not currently being considered for publication elsewhere. We confirm that the manuscript has been read and approved by all named authors and that there are no other persons who satisfied the criteria for authorship but are not listed. We further confirm that the order of authors listed in the manuscript has been approved by all of us.

Fardeen Shakur Athoye: Data Curation, Formal analysis, Investigation, Methodology, Software, Visualization, Writing – original draft, Writing - review & editing. **Dr. Mohammad Shakil Akther:** Conceptualization, Methodology, Supervision, Writing - review & editing.

References

[1] S. Grimmond, "Urbanization and Global Environmental Change: Local Effects of Urban Warming," *Geogr. J.*, vol. 173, no. 1, pp. 83–88, 2007, [Online]. Available: http://www.jstor.org/stable/30113496.

[2] United Nations, Department of Economic and Social Affairs, Population Division, "World Urbanization Prospects," United Nations, Department of Economic and Social Affairs, Population Division, New York, ST/ESA/SER.A/420, 2019. Accessed: Feb. 28, 2024. [Online]. Available: https://population.un.org/wup/assets/WUP2018-Report.pdf

[3] A. M. Rizwan, L. Y. C. Dennis, and C. Liu, "A review on the generation, determination and mitigation of Urban Heat Island," *J. Environ. Sci.*, vol. 20, no. 1, pp. 120–128, Jan. 2008, doi: 10.1016/S1001-0742(08)60019-4.

[4] S. Wang, S. Gao, S. Li, and K. Feng, "Strategizing the relation between urbanization and air pollution: Empirical evidence from global countries," *J. Clean. Prod.*, vol. 243, p. 118615, Jan. 2020, doi: 10.1016/j.jclepro.2019.118615.

[5] A. T. Anastasopolos *et al.*, "Air quality in Canadian port cities after regulation of low-sulphur marine fuel in the North American Emissions Control Area," *Sci. Total Environ.*, vol. 791, p. 147949, Oct. 2021, doi: 10.1016/j.scitotenv.2021.147949.

[6] V. Fioletov *et al.*, "Multi-source SO_2 emission retrievals and consistency of satellite and surface measurements with reported emissions," *Atmospheric Chem. Phys.*, vol. 17, no. 20, pp. 12597–12616, Oct. 2017, doi: 10.5194/acp-17-12597-2017.

[7] N. A. Krotkov *et al.*, "Aura OMI observations of regional SO_2 and NO_2 pollution changes from 2005 to 2015," *Atmospheric Chem. Phys.*, vol. 16, no. 7, pp. 4605–4629, Apr. 2016, doi: 10.5194/acp-16-4605-2016.

[8] B. F. O'Leary *et al.*, "Air quality monitoring and measurement in an urban airshed: Contextualizing datasets from the Detroit Michigan area from 1952 to 2020," *Sci. Total Environ.*, vol. 809, p. 152120, Feb. 2022, doi: 10.1016/j.scitotenv.2021.152120.

[9] C. Li, M. S. Hammer, B. Zheng, and R. C. Cohen, "Accelerated reduction of air pollutants in China, 2017-2020," *Sci. Total Environ.*, vol. 803, p. 150011, Jan. 2022, doi: 10.1016/j.scitotenv.2021.150011.

[10] X. Liu *et al.*, "Evaluating cost and benefit of air pollution control policies in China: A systematic review," *J. Environ. Sci.*, vol. 123, pp. 140–155, Jan. 2023, doi: 10.1016/j.jes.2022.02.043.

[11] P. Thangavel, D. Park, and Y.-C. Lee, "Recent Insights into Particulate Matter (PM2.5)-Mediated Toxicity in Humans: An Overview," *Int. J. Environ. Res. Public. Health*, vol. 19, no. 12, p. 7511, Jun. 2022, doi: 10.3390/ijerph19127511.

[12] World Bank, "Striving for Clean Air: Air Pollution and Public Health in South Asia," The World Bank, Washington, DC, Jun. 2023. doi: 10.1596/978-1-4648-1831-8.

[13] M. M. Rahman, S. Mahamud, and G. D. Thurston, "Recent spatial gradients and time trends in Dhaka, Bangladesh, air pollution and their human health implications," *J. Air Waste Manag. Assoc.*, vol. 69, no. 4, pp. 478–501, Apr. 2019, doi: 10.1080/10962247.2018.1548388.

[14] M. H. Rahman and A. Al-Muyeed, "Urban air pollution: a Bangladesh perspective," presented at the WIT Transactions on Ecology and the Environment, WIT Press, Jan. 2005, pp. 605–614. doi: DOI:10.2495/AIR050611.

[15] Md. M. Islam, M. Sharmin, and F. Ahmed, “Predicting air quality of Dhaka and Sylhet divisions in Bangladesh: a time series modeling approach,” *Air Qual. Atmosphere Health*, vol. 13, no. 5, pp. 607–615, May 2020, doi: 10.1007/s11869-020-00823-9.

[16] D. Rodríguez-Urrego and L. Rodríguez-Urrego, “Air quality during the COVID-19: PM2.5 analysis in the 50 most polluted capital cities in the world,” *Environ. Pollut.*, vol. 266, p. 115042, Nov. 2020, doi: 10.1016/j.envpol.2020.115042.

[17] Md. M. Rana and Dr. S. K. Biswas, “Ambient Air Quality in Bangladesh,” Department of Environment, Ministry of Environment, Forest and Climate Change of the Government of Bangladesht, Bangladesh, Sep. 2018. [Online]. Available: https://doe.portal.gov.bd/sites/default/files/files/doe.portal.gov.bd/page/cdbe516f_1756_426f_af6b_3ae9f35a78a4/2020-06-13-16-41-3d93aa7bc8290680d3fc447f257c421b.pdf

[18] AQI.in, “Worldwide Air Quality Report 2024,” Feb. 2025. Accessed: Mar. 19, 2025. [Online]. Available: https://www.aqi.in/world-air-quality-report

[19] Department of Environment (DoE), “Daily Air Quality Index (AQI) Report,” E-16, Agargaon, Sher-e-Bangla Nagar, Dhaka, Jan. 2025. Accessed: Feb. 19, 2025. [Online]. Available: https://doe.portal.gov.bd/sites/default/files/files/doe.portal.gov.bd/page/cd3cce3e_c23b_4321_a525_4461e497120a/2025-01-26-03-22-81b40f6cb20cdddec9e69b3358b59abd.pdf

[20] Department of Environment (DoE), “Air Quality Monthly Report,” Department of Environment, Ministry of Environment and Forests, Government of the People’s Republic of Bangladesh, Feb. 2025. Accessed: Feb. 19, 2025. [Online]. Available: https://doe.portal.gov.bd/sites/default/files/files/doe.portal.gov.bd/page/4e37d9e4_c6e5_4767_9905_f92f52cd557e/2025-03-20-06-50-1151335b217af6f03f20a57b8780b0b6.pdf

[21] A. P. Dadhich, R. Goyal, and P. N. Dadhich, “Assessment of spatio-temporal variations in air quality of Jaipur city, Rajasthan, India,” *Egypt. J. Remote Sens. Space Sci.*, vol. 21, no. 2, pp. 173–181, Sep. 2018, doi: 10.1016/j.ejrs.2017.04.002.

[22] W. Fu *et al.*, “Spatial and Temporal Variations of Six Criteria Air Pollutants in Fujian Province, China,” *Int. J. Environ. Res. Public. Health*, vol. 15, no. 12, p. 2846, Dec. 2018, doi: 10.3390/ijerph15122846.

[23] K. Gupta, A. Saha, and B. Sen Gupta, “Spatio-temporal distribution of pollutant trace gases (CO, CH_4 , O_3 and NO_2) in India: an observational study,” *Geol. Ecol. Landsc.*, vol. 8, no. 3, pp. 306–326, Jul. 2024, doi: 10.1080/24749508.2022.2132706.

[24] M. Kuerban *et al.*, “Spatio-temporal patterns of air pollution in China from 2015 to 2018 and implications for health risks,” *Environ. Pollut.*, vol. 258, p. 113659, Mar. 2020, doi: 10.1016/j.envpol.2019.113659.

[25] C. Nanda, Y. Kant, A. Gupta, and D. Mitra, “Spatio-temporal Distribution of Pollutant Trace Gases During Diwali Over India,” *ISPRS Ann. Photogramm. Remote Sens. Spat. Inf. Sci.*, vol. IV–5, pp. 339–350, Nov. 2018, doi: 10.5194/isprs-annals-IV-5-339-2018.

[26] H. R. Naqvi, G. Mutreja, A. Shakeel, and M. A. Siddiqui, “Spatio-temporal analysis of air quality and its relationship with major COVID-19 hotspot places in India,” *Remote Sens. Appl. Soc. Environ.*, vol. 22, p. 100473, Apr. 2021, doi: 10.1016/j.rsase.2021.100473.

[27] Y. Tui, J. Qiu, J. Wang, and C. Fang, “Analysis of Spatio-Temporal Variation Characteristics of Main Air Pollutants in Shijiazhuang City,” *Sustainability*, vol. 13, no. 2, p. 941, Jan. 2021, doi: 10.3390/su13020941.

[28] C. Zhao *et al.*, “Spatio-temporal analysis of urban air pollutants throughout China during 2014–2019,” *Air Qual. Atmosphere Health*, vol. 14, no. 10, pp. 1619–1632, Oct. 2021, doi: 10.1007/s11869-021-01043-5.

[29] S. Zhao, Y. Yu, D. Yin, D. Qin, J. He, and L. Dong, “Spatial patterns and temporal variations of six criteria air pollutants during 2015 to 2017 in the city clusters of Sichuan Basin, China,” *Sci. Total Environ.*, vol. 624, pp. 540–557, May 2018, doi: 10.1016/j.scitotenv.2017.12.172.

[30] Md. O. Rahaman, K. Roksana, and M. K. Mukit, “Spatial and Temporal Trends of Air Quality around Dhaka City: A GIS Approach,” *Adv. Appl. Sci. Res.*, vol. 11, no. 4, p. 8, Oct. 2024, Accessed: Mar. 14, 2025. [Online]. Available: https://www.researchgate.net/publication/359033089_Spatial_and_Temporal_Trends_of_Air_Quality_around_Dhaka_City_A_GIS_Approach

[31] N. Islam, T. R. Toha, M. M. Islam, and T. Ahmed, "Spatio-temporal Variation of Meteorological Influence on PM2.5 and PM10 over Major Urban Cities of Bangladesh," *Aerosol Air Qual. Res.*, vol. 23, no. 1, p. 220082, 2023, doi: 10.4209/aaqr.220082.

[32] B. A. Begum and P. K. Hopke, "Ambient Air Quality in Dhaka Bangladesh over Two Decades: Impacts of Policy on Air Quality," *Aerosol Air Qual. Res.*, vol. 18, no. 7, pp. 1910–1920, 2018, doi: 10.4209/aaqr.2017.11.0465.

[33] Department of Environment (DoE), "National Strategy For Sustainable Brick Production in Bangladesh," Department of Environment, Ministry of Environment and Forests, Government of the People's Republic of Bangladesh, May 2017. Accessed: Mar. 06, 2024. [Online]. Available: https://www.ccacoalition.org/sites/default/files/resources/2017_strategy-brick-production-bangladesh.pdf

[34] S. N. Rahaman *et al.*, "A Multivariate Geostatistical Framework to Assess the Spatio-Temporal Dynamics of Air Pollution and Land Surface Temperature in Bangladesh," *Earth Syst. Environ.*, vol. 9, no. 1, pp. 71–91, Jan. 2025, doi: 10.1007/s41748-024-00418-9.

[35] N. Shobnom, S. Hossain, and R. Roni, "Monitoring spatiotemporal changes of NO2 using TROPOMI and sentinel-5 images for Dhaka city and its surrounding areas of Bangladesh," *J. Air Pollut. Health*, Oct. 2023, doi: 10.18502/japh.v8i3.13785.

[36] K. Cai *et al.*, "Spatio-temporal Variations in NO2 and PM2.5 over the Central Plains Economic Region of China during 2005-2015 Based on Satellite Observations," *Aerosol Air Qual. Res.*, vol. 18, no. 5, pp. 1221–1235, 2018, doi: 10.4209/aaqr.2017.10.0394.

[37] Md. S. Hassan, R. F. L. Gomes, M. A. H. Bhuiyan, and M. T. Rahman, "Land Use and the Climatic Determinants of Population Exposure to PM2.5 in Central Bangladesh," *Pollutants*, vol. 3, no. 3, pp. 381–395, Aug. 2023, doi: 10.3390/pollutants3030026.

[38] M. M. Rahman, S. Wang, W. Zhao, A. Arshad, W. Zhang, and C. He, "Comprehensive Evaluation of Spatial Distribution and Temporal Trend of NO2, SO2 and AOD Using Satellite Observations over South and East Asia from 2011 to 2021," *Remote Sens.*, vol. 15, no. 20, p. 5069, Oct. 2023, doi: 10.3390/rs15205069.

[39] J. R. Mitra and K. Czajkowski, "Spatiotemporal patterns and hot spots of PM2.5 in Bangladesh," *Atmospheric Res.*, vol. 315, p. 107898, Apr. 2025, doi: 10.1016/j.atmosres.2024.107898.

[40] R.-R. Rahman and A. Kabir, "Spatiotemporal analysis and forecasting of air quality in the greater Dhaka region and assessment of a novel particulate matter filtration unit," *Environ. Monit. Assess.*, vol. 195, no. 7, p. 824, Jul. 2023, doi: 10.1007/s10661-023-11370-y.

[41] A. Mathew *et al.*, "Unveiling urban air quality dynamics during COVID-19: a Sentinel-5P TROPOMI hotspot analysis," *Sci. Rep.*, vol. 14, no. 1, p. 21624, Sep. 2024, doi: 10.1038/s41598-024-72276-4.

[42] B. A. Begum, S. K. Biswas, and P. K. Hopke, "Temporal variations and spatial distribution of ambient PM2.2 and PM10 concentrations in Dhaka, Bangladesh," *Sci. Total Environ.*, vol. 358, no. 1–3, pp. 36–45, Apr. 2006, doi: 10.1016/j.scitotenv.2005.05.031.

[43] M. S. Islam, S. Roy, T. R. Tusher, M. Rahman, and R. C. Harris, "Assessment of Spatio-Temporal Variations in PM2.5 and Associated Long-Range Air Mass Transport and Mortality in South Asia," *Remote Sens.*, vol. 15, no. 20, p. 4975, Oct. 2023, doi: 10.3390/rs15204975.

[44] M. S. Islam, T. R. Tusher, S. Roy, and M. Rahman, "Impacts of nationwide lockdown due to COVID-19 outbreak on air quality in Bangladesh: a spatiotemporal analysis," *Air Qual. Atmosphere Health*, vol. 14, no. 3, pp. 351–363, Mar. 2021, doi: 10.1007/s11869-020-00940-5.

[45] M. M. Islam and S. Afrin, "AIR QUALITY STATUS OF DHAKA CITY AND EFFECTS OF SEASONS, WEEKENDS, EID AND HARTAL DAYS," in *2nd International Conference on Advances in Civil Engineering 2014 (ICACE-2014)*, CUET, Chittagong, Bangladesh, Dec. 2015. Accessed: Mar. 14, 2025. [Online]. Available: https://www.academia.edu/39869872/AIR_QUALITY_STATUS_OF_DHAKA_CITY_AND_EFFECTS_OF_SEASONS_WEEKENDS_EID_AND_HARTAL_DAYS

[46] A. Ahmed, A. A. Bin Ali, M. Mahboob, and F. Humaira, "Comparison between Local and Global Methods to Develop AQI in Representing the Spatial Pattern of Air Quality of Dhaka City," *Dhaka Univ. J. Earth Environ. Sci.*, vol. 11, no. 1, pp. 131–149, Feb. 2023, doi: 10.3329/dujees.v11i1.63716.

[47] Dhaka South City Corporation, “At A Glance Dhaka South City Corporation,” Bangladesh National Portal. Accessed: Mar. 14, 2024. [Online]. Available: https://dscc.gov.bd/site/page/c918f990-1f75-46cb-95ad-c08d10197af5/-
[48] Dhaka North City Corporation, “Location and Area,” Bangladesh National Portal.
[49] Bangladesh Bureau of Statistics, “Population and Housing Census 2022,” Bangladesh Bureau of Statistics, Statistics and Informatics Division, Ministry of Planning, Jun. 2024. Accessed: Mar. 12, 2025. [Online]. Available: http://203.112.218.101/storage/files/1/Publications/PHCensus/Dhaka/District%20Report%20Dhaka.pdf
[50] S. N. Rahaman, S. M. M. Ahmed, M. Zeyad, and A. H. Zim, “Effect of vegetation and land surface temperature on NO2 concentration: A Google Earth Engine-based remote sensing approach,” *Urban Clim.*, vol. 47, p. 101336, Jan. 2023, doi: 10.1016/j.uclim.2022.101336.
[51] World Health Organization, “WHO’s Urban Ambient Air Pollution database - Update 2016.” 2016. Accessed: Mar. 12, 2025. [Online]. Available: https://cdn.who.int/media/docs/default-source/air-quality-database/aqd-2016/aap_database_summary_results_2016_v02.pdf?sfvrsn=384beb23_3
[52] H. Du *et al.*, “Influences of land cover types, meteorological conditions, anthropogenic heat and urban area on surface urban heat island in the Yangtze River Delta Urban Agglomeration,” *Sci. Total Environ.*, vol. 571, pp. 461–470, Nov. 2016, doi: 10.1016/j.scitotenv.2016.07.012.
[53] D. Hashim and P. Boffetta, “Occupational and Environmental Exposures and Cancers in Developing Countries,” *Ann. Glob. Health*, vol. 80, no. 5, p. 393, Dec. 2014, doi: 10.1016/j.aogh.2014.10.002.
[54] S. Nasehi, A. Yavar, and E. Salehi, “Investigating the spatial distribution of land surface temperature as related to air pollution level in Tehran metropolis,” *Pollution*, vol. 9, no. 1, pp. 1–14, Nov. 2022, doi: http//doi.org/10.22059/POLL.2022.330381.1181.
[55] G. Suthar, N. Kaul, S. Khandelwal, and S. Singh, “Predicting land surface temperature and examining its relationship with air pollution and urban parameters in Bengaluru: A machine learning approach,” *Urban Clim.*, vol. 53, p. 101830, Jan. 2024, doi: 10.1016/j.uclim.2024.101830.
[56] Y. Wang, Z. Guo, and J. Han, “The relationship between urban heat island and air pollutants and them with influencing factors in the Yangtze River Delta, China,” *Ecol. Indic.*, vol. 129, p. 107976, Oct. 2021, doi: 10.1016/j.ecolind.2021.107976.
[57] R. Kumar *et al.*, “How Will Air Quality Change in South Asia by 2050?,” *J. Geophys. Res. Atmospheres*, vol. 123, no. 3, pp. 1840–1864, Feb. 2018, doi: 10.1002/2017JD027357.
[58] O. Schneising *et al.*, “A scientific algorithm to simultaneously retrieve carbon monoxide and methane from TROPOMI onboard Sentinel-5 Precursor,” *Atmospheric Meas. Tech.*, vol. 12, no. 12, pp. 6771–6802, Dec. 2019, doi: 10.5194/amt-12-6771-2019.
[59] K. Fuladlu and H. Altan, “Examining land surface temperature and relations with the major air pollutants: A remote sensing research in case of Tehran,” *Urban Clim.*, vol. 39, p. 100958, Sep. 2021, doi: 10.1016/j.uclim.2021.100958.
[60] B. R. Parida *et al.*, “Improvement in air quality and its impact on land surface temperature in major urban areas across India during the first lockdown of the pandemic,” *Environ. Res.*, vol. 199, p. 111280, Aug. 2021, doi: 10.1016/j.envres.2021.111280.
[61] P. Purwanto, I. S. Astuti, F. Rohman, K. S. B. Utomo, and Y. E. Aldianto, “Assessment of the dynamics of urban surface temperatures and air pollution related to COVID-19 in a densely populated City environment in East Java,” *Ecol. Inform.*, vol. 71, p. 101809, Nov. 2022, doi: 10.1016/j.ecoinf.2022.101809.
[62] Md. N. Islam and Md. P. Parvez, “Predicting the El Niño and La Niño impact on the coastal zones at the Bay of Bengal and the likelihood of weather patterns in Bangladesh,” *Model. Earth Syst. Environ.*, vol. 6, no. 3, pp. 1823–1839, Sep. 2020, doi: 10.1007/s40808-020-00793-y.
[63] M. H. R. Khan, A. Rahman, C. Luo, S. Kumar, G. M. A. Islam, and M. A. Hossain, “Detection of changes and trends in climatic variables in Bangladesh during 1988–2017,” *Heliyon*, vol. 5, no. 3, p. e01268, Mar. 2019, doi: 10.1016/j.heliyon.2019.e01268.

[64] Z. Qiu *et al.*, "Spatiotemporal Investigations of Multi-Sensor Air Pollution Data over Bangladesh during COVID-19 Lockdown," *Remote Sens.*, vol. 13, no. 5, p. 877, Feb. 2021, doi: 10.3390/rs13050877.

[65] M. S. Hammer *et al.*, "Global Estimates and Long-Term Trends of Fine Particulate Matter Concentrations (1998–2018)," *Environ. Sci. Technol.*, vol. 54, no. 13, pp. 7879–7890, Jul. 2020, doi: 10.1021/acs.est.0c01764.

[66] A. Van Donkelaar *et al.*, "Global Estimates of Fine Particulate Matter using a Combined Geophysical-Statistical Method with Information from Satellites, Models, and Monitors," *Environ. Sci. Technol.*, vol. 50, no. 7, pp. 3762–3772, Apr. 2016, doi: 10.1021/acs.est.5b05833.

[67] Md. S. Hassan and M. A. H. Bhuiyan, "Spatiotemporal Mapping and Modeling Hotspot of PM2.5 in the Central part of Bangladesh," *J. Hyperspectral Remote Sens.*, vol. 13, no. 1, pp. 13–23, Mar. 2023, doi: DOI:10.29150/2237-2202.2023.257250.

[68] D. Zhou, S. Bonafoni, L. Zhang, and R. Wang, "Remote sensing of the urban heat island effect in a highly populated urban agglomeration area in East China," *Sci. Total Environ.*, vol. 628–629, pp. 415–429, Jul. 2018, doi: 10.1016/j.scitotenv.2018.02.074.

[69] O. E. Adeyeri, A. A. Akinsanola, and K. A. Ishola, "Investigating surface urban heat island characteristics over Abuja, Nigeria: Relationship between land surface temperature and multiple vegetation indices," *Remote Sens. Appl. Soc. Environ.*, vol. 7, pp. 57–68, Aug. 2017, doi: 10.1016/j.rsase.2017.06.005.

[70] G. Nautiyal, S. Maithani, and A. Sharma, "Exploring the Relationship Between Spatio-temporal Land Cover Dynamics and Surface Temperature Over Dehradun Urban Agglomeration, India," *J. Indian Soc. Remote Sens.*, vol. 49, no. 6, pp. 1307–1318, Jun. 2021, doi: 10.1007/s12524-021-01323-8.

[71] R. C. Estoque, Y. Murayama, and S. W. Myint, "Effects of landscape composition and pattern on land surface temperature: An urban heat island study in the megacities of Southeast Asia," *Sci. Total Environ.*, vol. 577, pp. 349–359, Jan. 2017, doi: 10.1016/j.scitotenv.2016.10.195.

[72] O. Rozenstein, Z. Qin, Y. Derimian, and A. Karnieli, "Derivation of Land Surface Temperature for Landsat-8 TIRS Using a Split Window Algorithm," *Sensors*, vol. 14, no. 4, pp. 5768–5780, Mar. 2014, doi: 10.3390/s140405768.

[73] Y. J. Kaufman and D. Tanre, "Atmospherically resistant vegetation index (ARVI) for EOS-MODIS," *IEEE Trans. Geosci. Remote Sens.*, vol. 30, no. 2, pp. 261–270, Mar. 1992, doi: 10.1109/36.134076.

[74] J. Xue and B. Su, "Significant Remote Sensing Vegetation Indices: A Review of Developments and Applications," *J. Sens.*, vol. 2017, pp. 1–17, 2017, doi: 10.1155/2017/1353691.

[75] P. T. Grzybowski, K. M. Markowicz, and J. P. Musiał, "Estimations of the Ground-Level NO2 Concentrations Based on the Sentinel-5P NO2 Tropospheric Column Number Density Product," *Remote Sens.*, vol. 15, no. 2, p. 378, Jan. 2023, doi: 10.3390/rs15020378.

[76] S. S. Shapiro and M. B. Wilk, "An analysis of variance test for normality (complete samples)," *Biometrika*, vol. 52, no. 3–4, pp. 591–611, Dec. 1965, doi: 10.1093/biomet/52.3-4.591.

[77] I. P. Senanayake, W. D. D. P. Welivitiya, and P. M. Nadeeka, "Urban green spaces analysis for development planning in Colombo, Sri Lanka, utilizing THEOS satellite imagery – A remote sensing and GIS approach," *Urban For. Urban Green.*, vol. 12, no. 3, pp. 307–314, Jan. 2013, doi: 10.1016/j.ufug.2013.03.011.

[78] Sh. Faryadi and S. Taheri, "Interconnections of Urban Green Spaces and Environmental Quality of Tehran," *Int. J. Environ. Res.*, vol. 3, no. 2, pp. 199–208, Mar. 2009, Accessed: Mar. 14, 2025. [Online]. Available: https://www.researchgate.net/publication/27794436_Interconnections_of_Urban_Green_Spaces_and_Environmental_Quality_of_Tehran

[79] M. M. Rahman, M. M. Rahman, and M. Momotaz, "Environmental quality evaluation in Dhaka City Corporation – using satellite imagery," *Proc. Inst. Civ. Eng. - Urban Des. Plan.*, vol. 172, no. 1, pp. 13–25, Feb. 2019, doi: 10.1680/jurdp.17.00032.

[80] A. Hoque and Md. A. Hossen, "Variation of Ambient air Quality Scenario in Chittagong City: A Case Study of Air Pollution," *J. Civ. Constr. Environ. Eng.*, vol. 3, no. 1, p. 10, 2018, doi: 10.11648/j.jccee.20180301.13.

[81] M. Greenstone, T. Ganguly, C. Hasenkopf, N. Sharma, and H. Gautam, "Air Quality Life Index | 2024," 2024. Accessed: Mar. 01, 2025. [Online]. Available: https://aqli.epic.uchicago.edu/wp-content/uploads/2024/08/AQLI-2024-Report_English.pdf
[82] M. Shammi, Md. Bodrud-Doza, A. R. Md. T. Islam, and Md. M. Rahman, "Strategic assessment of COVID-19 pandemic in Bangladesh: comparative lockdown scenario analysis, public perception, and management for sustainability," *Environ. Dev. Sustain.*, vol. 23, no. 4, pp. 6148–6191, Apr. 2021, doi: 10.1007/s10668-020-00867-y.
[83] J. M. Baldasano, "COVID-19 lockdown effects on air quality by NO2 in the cities of Barcelona and Madrid (Spain)," *Sci. Total Environ.*, vol. 741, p. 140353, Nov. 2020, doi: 10.1016/j.scitotenv.2020.140353.
[84] A. Agarwal, A. Kaushik, S. Kumar, and R. K. Mishra, "Comparative study on air quality status in Indian and Chinese cities before and during the COVID-19 lockdown period," *Air Qual. Atmosphere Health*, vol. 13, no. 10, pp. 1167–1178, Oct. 2020, doi: 10.1007/s11869-020-00881-z.
[85] S. Mahato, S. Pal, and K. G. Ghosh, "Effect of lockdown amid COVID-19 pandemic on air quality of the megacity Delhi, India," *Sci. Total Environ.*, vol. 730, p. 139086, Aug. 2020, doi: 10.1016/j.scitotenv.2020.139086.
[86] N. Sahani, S. K. Goswami, and A. Saha, "The impact of COVID-19 induced lockdown on the changes of air quality and land surface temperature in Kolkata city, India," *Spat. Inf. Res.*, vol. 29, no. 4, pp. 519–534, Aug. 2021, doi: 10.1007/s41324-020-00372-4.
[87] G. Dantas, B. Siciliano, B. B. França, C. M. Da Silva, and G. Arbilla, "The impact of COVID-19 partial lockdown on the air quality of the city of Rio de Janeiro, Brazil," *Sci. Total Environ.*, vol. 729, p. 139085, Aug. 2020, doi: 10.1016/j.scitotenv.2020.139085.
[88] S. Sharma, M. Zhang, Anshika, J. Gao, H. Zhang, and S. H. Kota, "Effect of restricted emissions during COVID-19 on air quality in India," *Sci. Total Environ.*, vol. 728, p. 138878, Aug. 2020, doi: 10.1016/j.scitotenv.2020.138878.
[89] X. Shi and G. P. Brasseur, "The Response in Air Quality to the Reduction of Chinese Economic Activities During the COVID-19 Outbreak," *Geophys. Res. Lett.*, vol. 47, no. 11, p. e2020GL088070, Jun. 2020, doi: 10.1029/2020GL088070.
[90] S. M. S. Rana, S. M. F. Ahmed, and H. Akter, "Analysis of NO2 Pollution over Bangladesh between the Two COVID-19 Caused Lockdowns in 2020 and 2021 Using Sentinel-5P Products," in *The 2nd International Electronic Conference on Applied Sciences*, MDPI, Oct. 2021, p. 30. doi: 10.3390/ASEC2021-11139.
[91] P. Wang, K. Chen, S. Zhu, P. Wang, and H. Zhang, "Severe air pollution events not avoided by reduced anthropogenic activities during COVID-19 outbreak," *Resour. Conserv. Recycl.*, vol. 158, p. 104814, Jul. 2020, doi: 10.1016/j.resconrec.2020.104814.
[92] R. Bao and A. Zhang, "Does lockdown reduce air pollution? Evidence from 44 cities in northern China," *Sci. Total Environ.*, vol. 731, p. 139052, Aug. 2020, doi: 10.1016/j.scitotenv.2020.139052.
[93] L. Li *et al.*, "Air quality changes during the COVID-19 lockdown over the Yangtze River Delta Region: An insight into the impact of human activity pattern changes on air pollution variation," *Sci. Total Environ.*, vol. 732, p. 139282, Aug. 2020, doi: 10.1016/j.scitotenv.2020.139282.
[94] M. C. Collivignarelli, A. Abbà, G. Bertanza, R. Pedrazzani, P. Ricciardi, and M. Carnevale Miino, "Lockdown for CoViD-2019 in Milan: What are the effects on air quality?," *Sci. Total Environ.*, vol. 732, p. 139280, Aug. 2020, doi: 10.1016/j.scitotenv.2020.139280.
[95] S. A. Abdul-Wahab and W. S. Bouhamra, "DIURNAL VARIATIONS OF AIR POLLUTION FROM MOTOR VEHICLES IN RESIDENTIAL AREA," *Int. J. Environ. Stud.*, vol. 61, no. 1, pp. 73–98, Feb. 2004, doi: 10.1080/0020723032000130034.
[96] L. Sahu and S. Lal, "Distributions of C2–C5 NMHCs and related trace gases at a tropical urban site in India," *Atmos. Environ.*, vol. 40, no. 5, pp. 880–891, Feb. 2006, doi: 10.1016/j.atmosenv.2005.10.021.
[97] M. R. S. Pavel, S. U. Zaman, F. Jeba, M. S. Islam, and A. Salam, "Long-Term (2003–2019) Air Quality, Climate Variables, and Human Health Consequences in Dhaka, Bangladesh," *Front. Sustain. Cities*, vol. 3, p. 681759, Jul. 2021, doi: 10.3389/frsc.2021.681759.

[98] J. Zhao, X. Wang, H. Song, Y. Du, W. Cui, and Y. Zhou, “Spatiotemporal Trend Analysis of PM2.5 Concentration in China, 1999–2016,” *Atmosphere*, vol. 10, no. 8, p. 461, Aug. 2019, doi: 10.3390/atmos10080461.
[99] M. Kandlikar and G. Ramachandran, “The causes and consequences of particulate air pollution in urban India: A synthesis of the science,” *Annu. Rev. Energy Environ.*, vol. 25, no. 1, pp. 629–684, Nov. 2000, doi: 10.1146/annurev.energy.25.1.629.
[100] T. T. N. Nguyen, H. A. Le, T. M. T. Mac, and N. T. T. Nhung, “Current Status of PM2.5 Pollution and its Mitigation in Vietnam,” *Glob. Environ. Res.*, vol. 22, no. 1 & 2, Oct. 2018, [Online]. Available: http://eprints.uet.vnu.edu.vn/eprints/id/eprint/3129
[101] M. Al-Hamdan, W. Crosson, E. Burrows, S. Coffield, B. Crane, and M. Barik, “Development and validation of improved PM2.5 models for public health applications using remotely sensed aerosol and meteorological data,” *Environ. Monit. Assess.*, vol. 191, no. S2, p. 328, Jun. 2019, doi: 10.1007/s10661-019-7414-3.
[102] M. A. Motalib and R. D. Lasco, “Assessing Air Quality in Dhaka City,” *Int. J. Sci. Res.*, vol. 4, no. 12, pp. 1908–1912, Dec. 2015, [Online]. Available: https://www.ijsr.net/archive/v4i12/SUB159291.pdf
[103] M. A.-M. Molla, “Nitrogen Dioxide: A growing health hazard for Dhaka,” *The Daily Star*, Bangladesh, Sep. 13, 2023. Accessed: Jun. 02, 2024. [Online]. Available: https://www.thedailystar.net/news/bangladesh/news/nitrogen-dioxide-growing-health-hazard-dhaka-3417286
[104] Bangladesh Road Transport Authority, “Number of Registered Motor Vehicles in Bangladesh (Yearwise)s,” 2024. Accessed: Jan. 10, 2025. [Online]. Available: https://brta.gov.bd/sites/default/files/files/brta.portal.gov.bd/page/6d849ccb_09aa_4fbe_aef2_3d254a2a0cd1/2024-02-13-06-58-00a465ab52ef0d35a090ca0610ebb75f.pdf
[105] A. Iqbal, S. Afroze, and Md. M. Rahman, “Probabilistic Health Risk Assessment of Vehicular Emissions as an Urban Health Indicator in Dhaka City,” *Sustainability*, vol. 11, no. 22, p. 6427, Nov. 2019, doi: 10.3390/su11226427.
[106] X. Guo *et al.*, “Air quality improvement and health benefit of PM2.5 reduction from the coal cap policy in the Beijing–Tianjin–Hebei (BTH) region, China,” *Environ. Sci. Pollut. Res.*, vol. 25, no. 32, pp. 32709–32720, Nov. 2018, doi: 10.1007/s11356-018-3014-y.
[107] D. J. Jacob and D. A. Winner, “Effect of climate change on air quality,” *Atmos. Environ.*, vol. 43, no. 1, pp. 51–63, Jan. 2009, doi: 10.1016/j.atmosenv.2008.09.051.
[108] M. P. George, B. J. Kaur, A. Sharma, and S. Mishra, “Seasonal Variation of Air Pollutants of Delhi and its Health Effects,” *NeBio J. Environ. Biodivers.*, vol. 4, no. 4, pp. 42–46, Aug. 2013.
[109] K. Karar and A. K. Gupta, “Seasonal variations and chemical characterization of ambient PM10 at residential and industrial sites of an urban region of Kolkata (Calcutta), India,” *Atmospheric Res.*, vol. 81, no. 1, pp. 36–53, Jul. 2006, doi: 10.1016/j.atmosres.2005.11.003.
[110] A. Kulshrestha, P. G. Satsangi, J. Masih, and A. Taneja, “Metal concentration of PM2.5 and PM10 particles and seasonal variations in urban and rural environment of Agra, India,” *Sci. Total Environ.*, vol. 407, no. 24, pp. 6196–6204, Dec. 2009, doi: 10.1016/j.scitotenv.2009.08.050.
[111] D. Sajan *et al.*, “Socioeconomic conditions and health hazards of brick field workers: A case study of Mymensingh brick industrial area of Bangladesh,” *J. Public Health Epidemiol.*, vol. 9, no. 7, pp. 198–205, Jul. 2017, doi: 10.5897/JPHE2017.0927.
[112] Dhaka Transport Coordination Board, “Preparatory Survey on Dhaka Urban Transport Network Development Study (DHUTS) Phase II,” Dhaka Transport Coordination Board, Ministry of Communications (MOC), Government of the People’s Republic of Bangladesh, Feb. 2011. Accessed: Jun. 02, 2024. [Online]. Available: https://openjicareport.jica.go.jp/pdf/11996782_07.pdf
[113] S. H. Rahman and M. Islam, “Urban Green-space Availability and Recommended Plantation Area in Dhaka South City Corporation (DSCC) using RS-GIS,” *Bangladesh J. Environ. Res.*, vol. 13, pp. 1–12, Jun. 2022.
[114] *Air Pollution Control Rules 2022*. 2022. Accessed: Jan. 01, 2025. [Online]. Available: https://file-mymensingh.portal.gov.bd/uploads/7d7d9b9e-d66f-4811-bc8b-ebea67523468//631/04a/85d/63104a85dba60724048427.pdf

[115] H. H. Suh, T. Bahadori, J. Vallarino, and J. D. Spengler, “Criteria air pollutants and toxic air pollutants.,” *Environ. Health Perspect.*, vol. 108, no. suppl 4, pp. 625–633, Aug. 2000, doi: 10.1289/ehp.00108s4625.

[116] J. W. S. Longhurst, S. J. Lindley, A. F. R. Watson, and D. E. Conlan, “The introduction of local air quality management in the United Kingdom: A review and theoretical framework,” *Atmos. Environ.*, vol. 30, no. 23, pp. 3975–3985, Dec. 1996, doi: 10.1016/1352-2310(96)00114-8.

[117] S. Gulia, S. M. S. Nagendra, J. Barnes, and M. Khare, “Urban local air quality management framework for non-attainment areas in Indian cities,” *Sci. Total Environ.*, vol. 619–620, pp. 1308–1318, Apr. 2018, doi: 10.1016/j.scitotenv.2017.11.123.